

Supporting Information for:

Translesion synthesis past the C8- and N²-deoxyguanosine adducts of the dietary mutagen 2-amino-3-methylimidazo[4,5-f]quinoline (IQ) in the *NarI* recognition sequence by bacterial DNA polymerases.

James S. Stover, Goutam Chowdhury, Hong Zang, F. Peter Guengerich and Carmelo J. Rizzo*

Departments of Chemistry and Biochemistry, Center in Molecular Toxicology, and Vanderbilt Institute of Chemical Biology, Vanderbilt University, Nashville, TN 37235-1822

Figure S1.	CGE analysis of oligonucleotide 1b .	3
Figure S2.	CGE analysis of oligonucleotide 1c .	3
Figure S3.	CGE analysis of oligonucleotide 2a .	4
Figure S4.	CGE analysis of oligonucleotide 2b .	4
Figure S5.	MALDI-TOF spectrum of oligonucleotide 1b .	5
Figure S6.	MALDI-TOF spectrum of oligonucleotide 1c .	5
Figure S7.	MALDI-TOF spectrum of oligonucleotide 2b .	6
Figure S8.	MALDI-TOF spectrum of oligonucleotide 2c .	6
Figure S9.	Single nucleotide incorporation of oligonucleotides 1a-c and 2a-c by Kf ⁻ .	7
Figure S10.	Single nucleotide incorporation of oligonucleotides 1b with a 0- and +1 primers.	8
Figure S11.	Single nucleotide incorporation of oligonucleotides 1a-c and 2a-c by pol II ⁻ .	9
Figure S12.	LC-ESI-MS/MS analysis of the pol II ⁻ extension of oligonucleotide 1b .	10
Figure S13.	TIC spectrum of the pol II ⁻ extension products from oligonucleotide 1b .	10
Figure S14.	CID spectrum of the <i>m/z</i> 944.07 products from the pol II ⁻ extension of oligonucleotide 1b .	11
Table S1.	Observed and calculated CID fragmentation of 5'-pGGCCGAGTT-3' (<i>m/z</i> 944.1).	11
Figure S15.	TIC (top) and CID (bottom) spectra of an authentic sample of 5'pGGCCGAGTT-3' (<i>m/z</i> 944.1).	12
Figure S16.	CID spectrum of the <i>m/z</i> 1053.7 products from the pol II ⁻ extension of oligonucleotide 1b .	13
Table S2.	Observed and calculated CID fragmentation of 5'-pGGGCCGAGTT-3' (<i>m/z</i> 1053.7).	13
Figure S17.	TIC (top) and CID (bottom) spectra of an authentic sample of 5'pGGGCCGAGTT-3' (<i>m/z</i> 1053.7).	14
Figure S18.	LC-ESI-MS/MS analysis of the pol II ⁻ extension of oligonucleotide 2b .	15

Figure S19.	TIC spectrum of the pol II ⁻ extension products from oligonucleotide 2b	15
Figure S20.	CID spectrum of the <i>m/z</i> 1152.8 products from the pol II ⁻ extension of oligonucleotide 2b	16
Table S3.	Observed and calculated CID fragmentation of 5'-pGGCGCCGAGTA-3' (<i>m/z</i> 1152.8).....	16
Figure S21.	TIC (top) and CID (bottom) spectra of an authentic sample of 5'-pGGCGCCGAGTA-3' (<i>m/z</i> 1052).....	17
Figure S22.	TIC spectrum of the pol II ⁻ extension of oligonucleotide 2c	18
Figure S23.	CID spectrum of the <i>m/z</i> 1048.7 product from the pol II ⁻ extension of oligonucleotide 2c	18
Table S4.	Observed and calculated CID fragmentation of 5'-pGGCGCCGAGT-3' (<i>m/z</i> 1048.7).....	19
Figure S24.	TIC (top) and CID (bottom) spectra of an authentic sample of 5'-pGGCGCCGAGT-3' (<i>m/z</i> 1048.7).....	20
Figure S25.	Single nucleotide incorporation of oligonucleotides 1a-c and 2a-c by Dpo4.....	21
Figure S26.	LC-ESI-MS/MS analysis of the Dpo4 extension of oligonucleotide 1b	22
Figure S26.	TIC spectrum of the Dpo4 extension products from oligonucleotide 1b	22
Figure S28.	CID spectrum of the <i>m/z</i> 1043.4 product from the Dpo4 extension of oligonucleotide 1b	23
Table S5.	Observed and calculated CID fragmentation of 5'-pGGCCCGCGAG-3' (<i>m/z</i> 1043.4).....	23
Figure S29.	TIC (top) and CID (bottom) spectra of an authentic sample of 5'-pGGCCCGCGAG-3' (<i>m/z</i> 1043.4).....	24
Figure S30.	LC-ESI-MS/MS analysis of the Dpo4 extension of oligonucleotide 2b	25
Figure S31.	TIC spectrum of the Dpo4 extension products from oligonucleotide 2b	25
Figure S32.	CID spectrum of the <i>m/z</i> 1048.5 products from the Dpo4 extension of oligonucleotide 2b	26
Table S6.	Observed and calculated CID fragmentation of 5'-pGGCGCCGAGT-3' (<i>m/z</i> 1048.5).....	26
Figure S33.	LC-ESI-MS/MS analysis of the Dpo4 extension of oligonucleotide 1c	27
Figure S34.	TIC spectrum of the Dpo4 extension products from oligonucleotide 1c	27
Figure S35.	CID spectrum of the <i>m/z</i> 1153.1 products from the Dpo4 extension of oligonucleotide 1c	28
Table S7.	Observed and calculated CID fragmentation of 5'-pGGCGCCGAGTA-3' (<i>m/z</i> 1153.1).....	28
Figure S36.	LC-ESI-MS/MS analysis of the Dpo4 extension of oligonucleotide 2c	29
Figure S37.	TIC spectrum of the Dpo4 extension products from oligonucleotide 2c	29
Figure S38.	CID spectrum of the <i>m/z</i> xxxx products from the Dpo4 extension of oligonucleotide 2b	30
Table S8.	Observed and calculated CID fragmentation of 5'-pGGCGCCGAGT-3' (<i>m/z</i> 1048.8).....	30

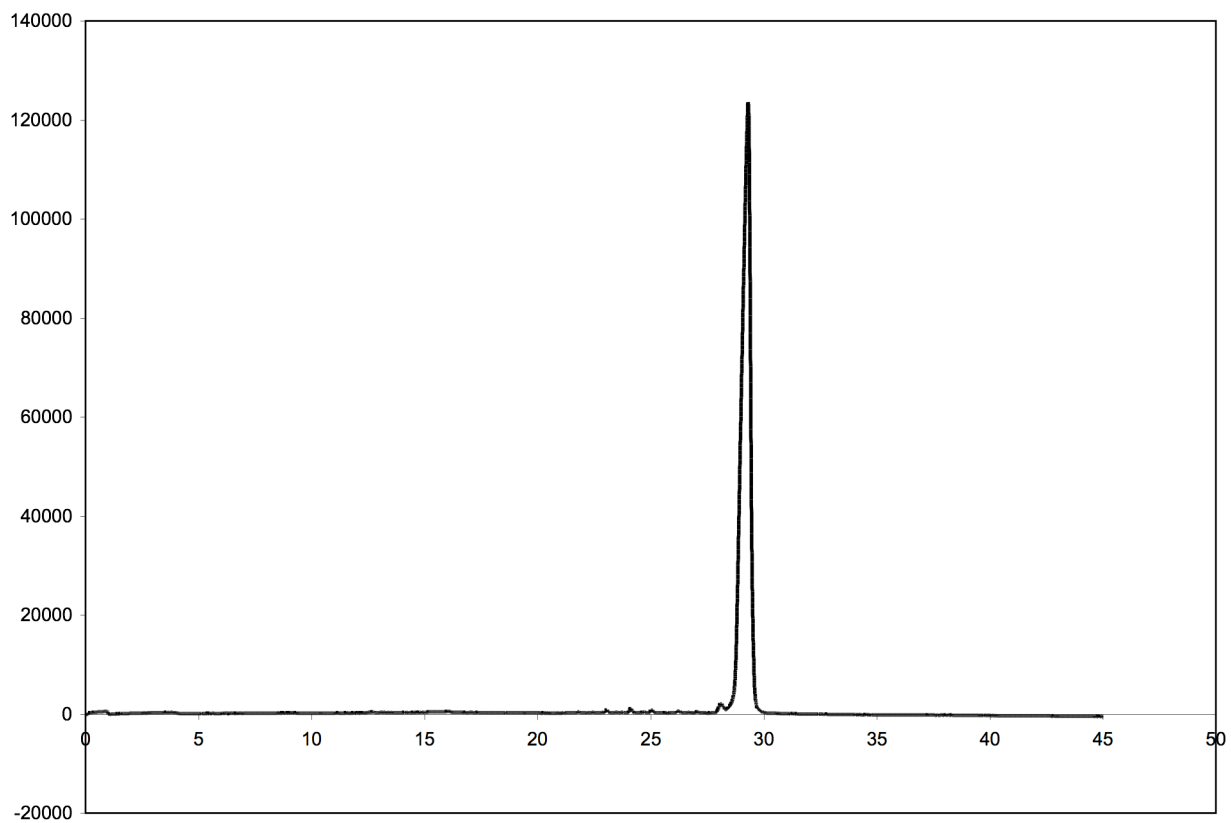


Figure S1. CGE analysis of oligonucleotide **1b**.

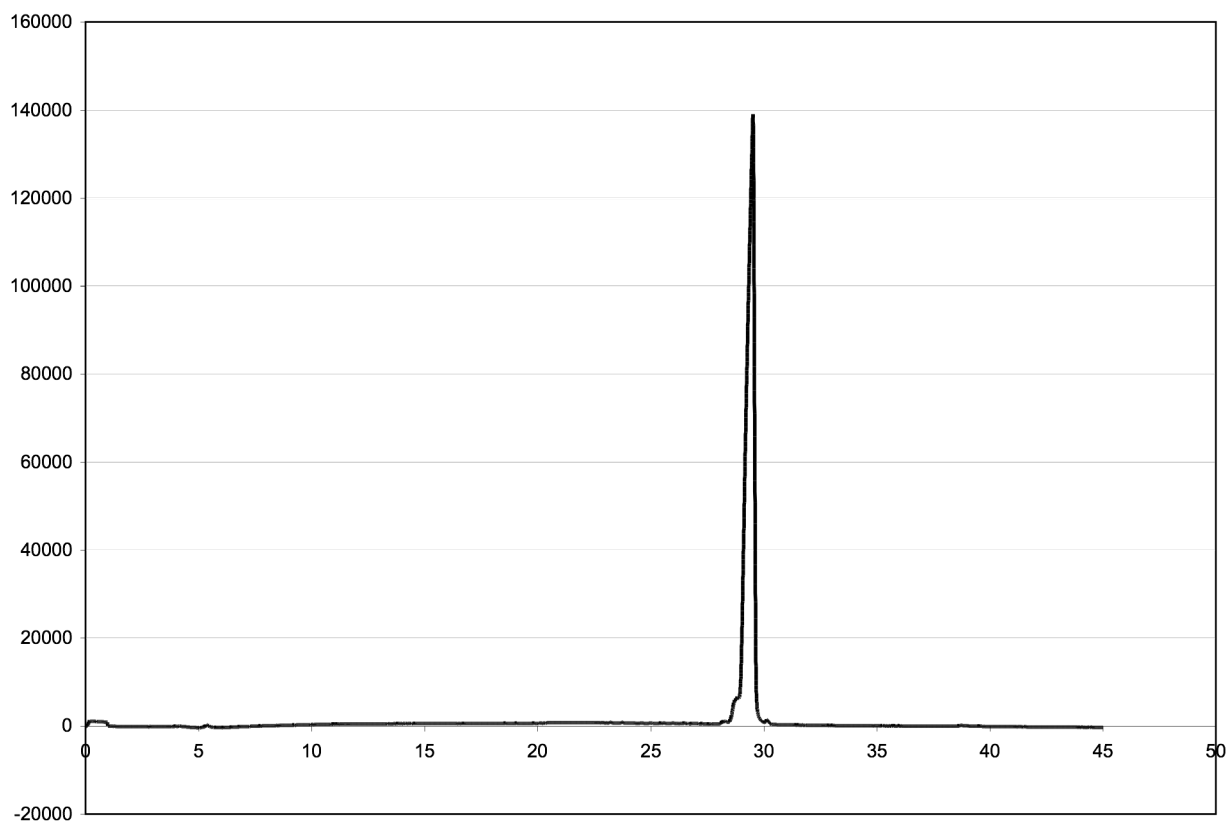


Figure S2. CGE analysis of oligonucleotide **1c**.

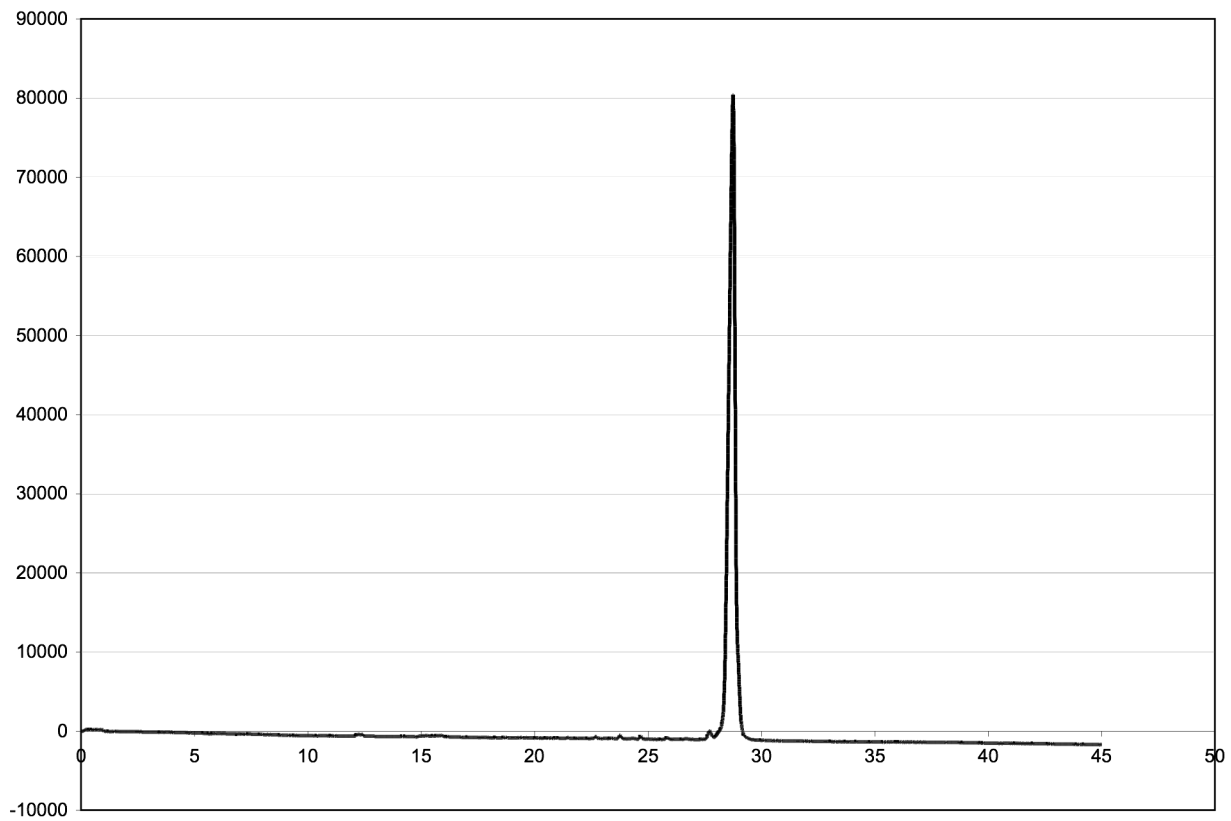


Figure S3. CGE analysis of oligonucleotide **2a**

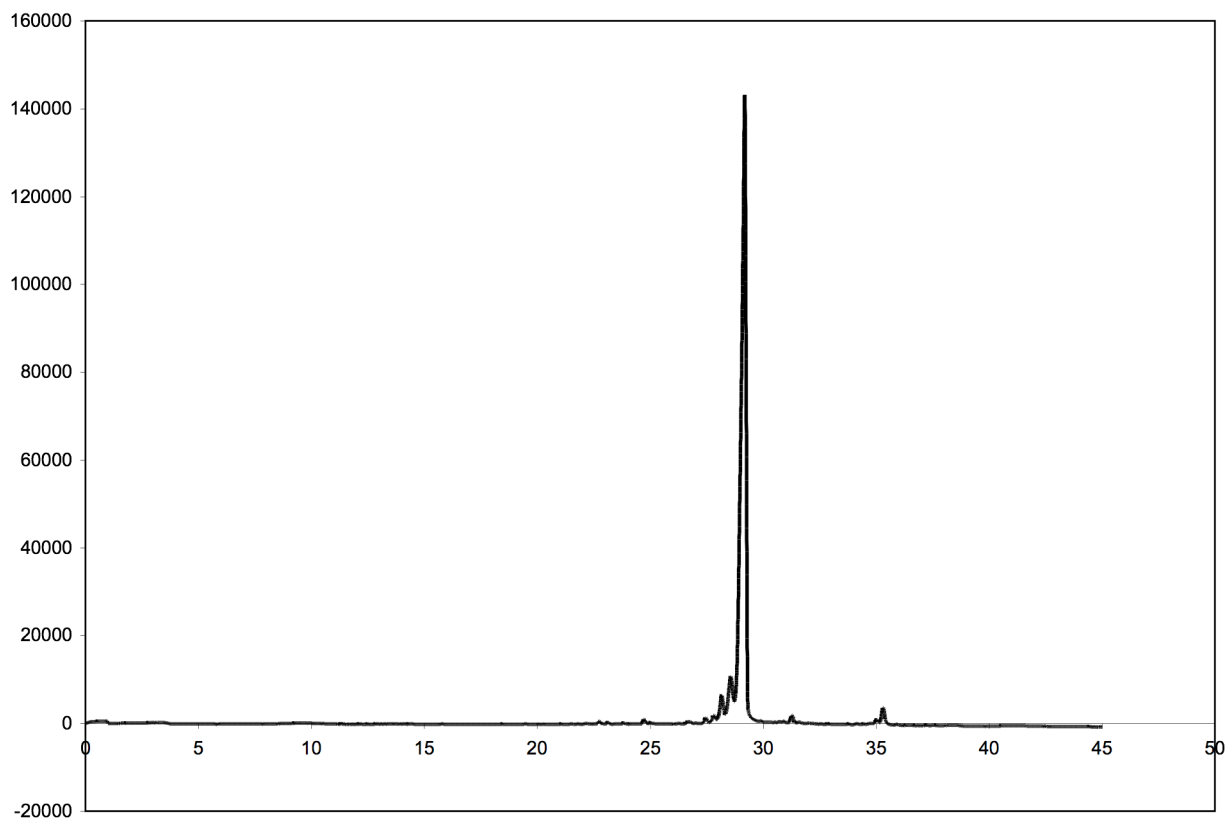


Figure S4. CGE analysis of oligonucleotide **2b**

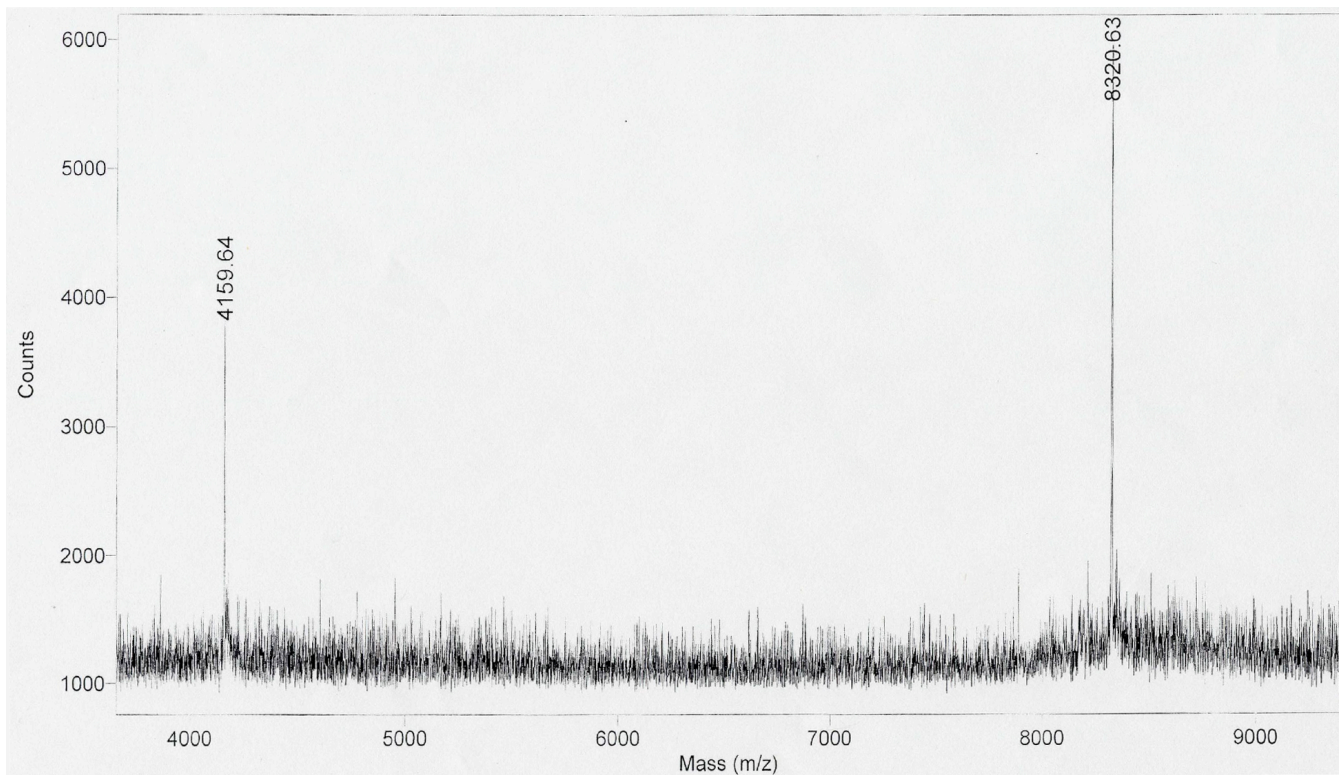


Figure S5. MALDI-TOF spectrum of oligonucleotide **1b**.

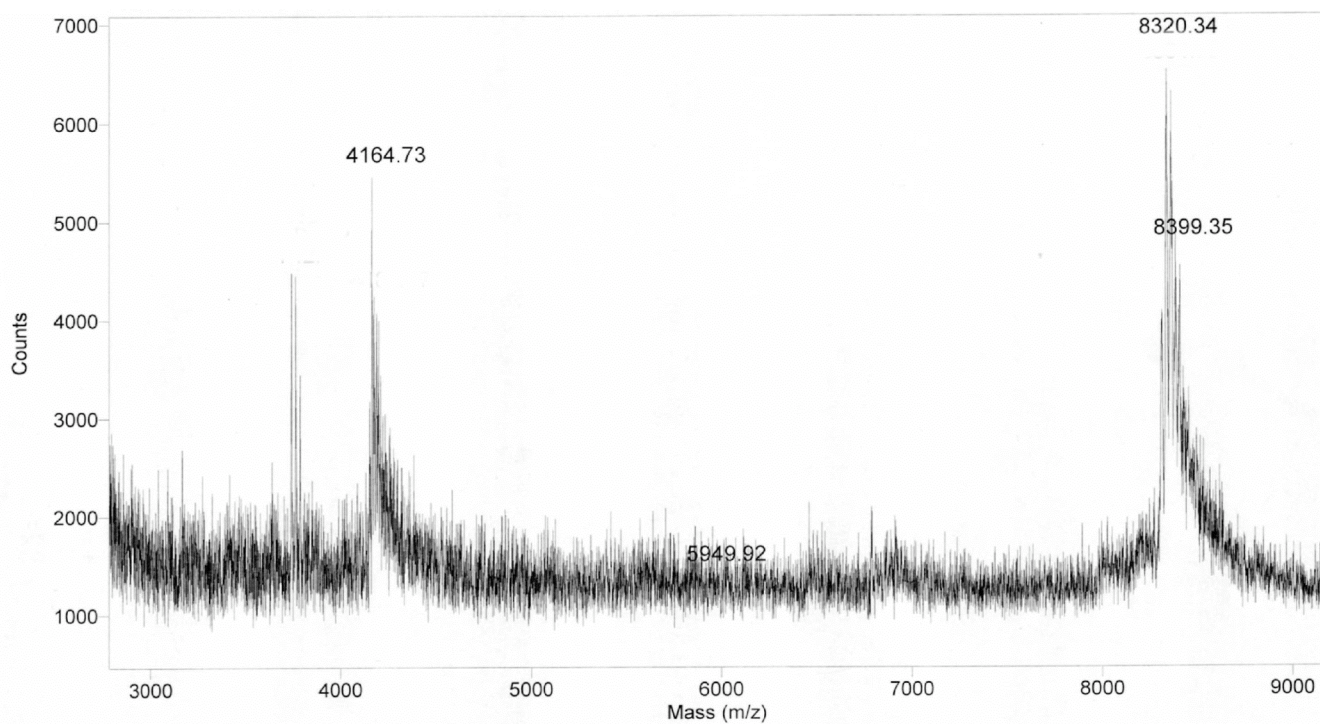


Figure S6. MALDI-TOF spectrum of oligonucleotide **1c**.

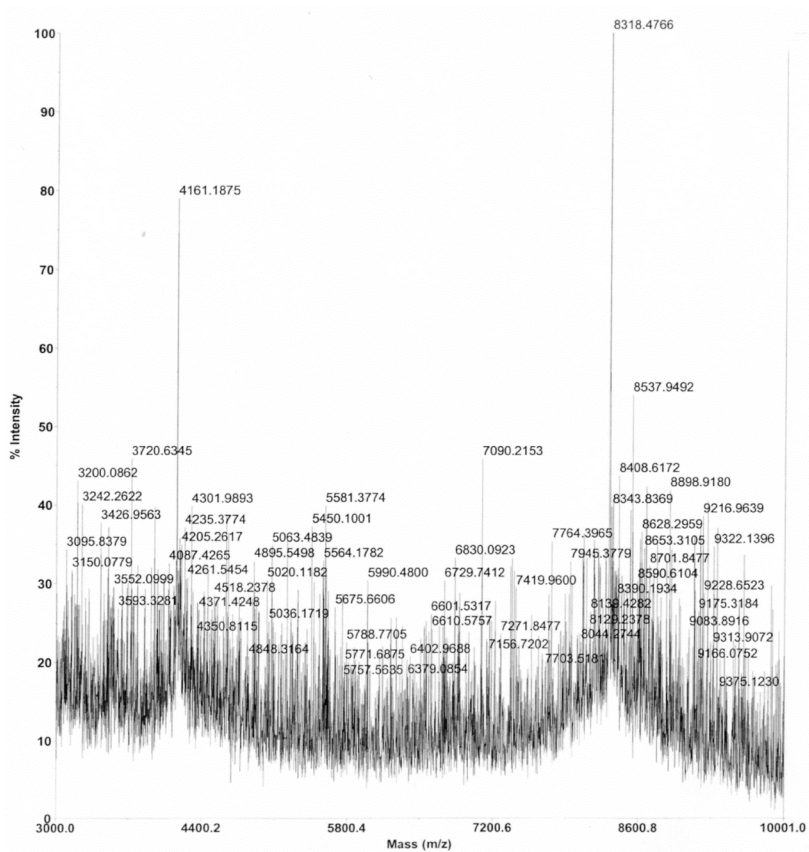


Figure S7. MALDI-TOF spectrum of oligonucleotide 2b.

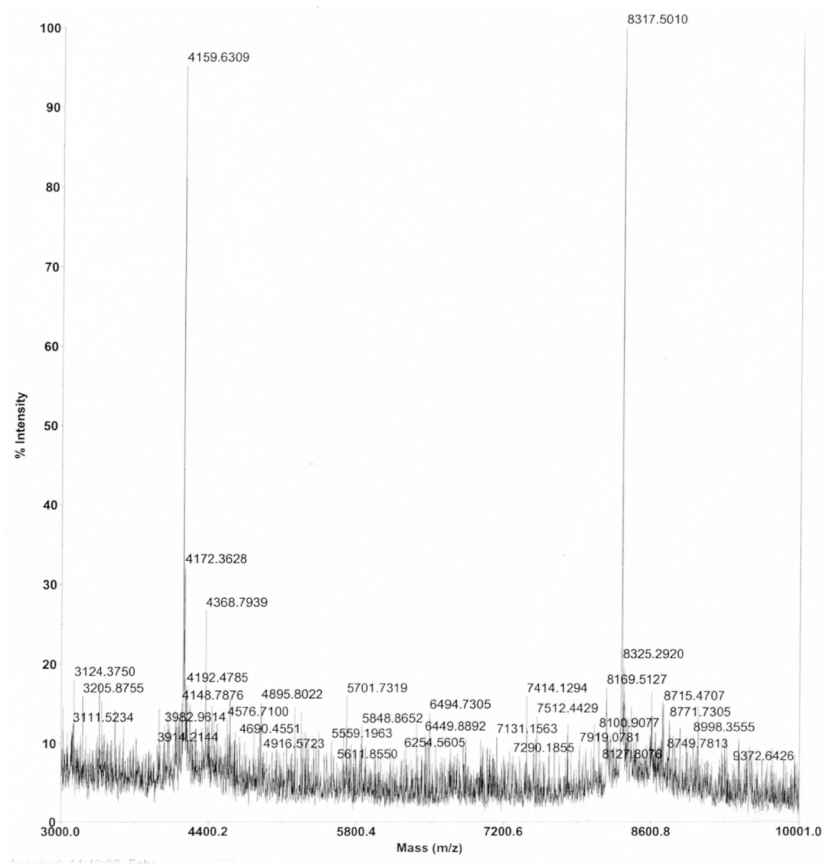
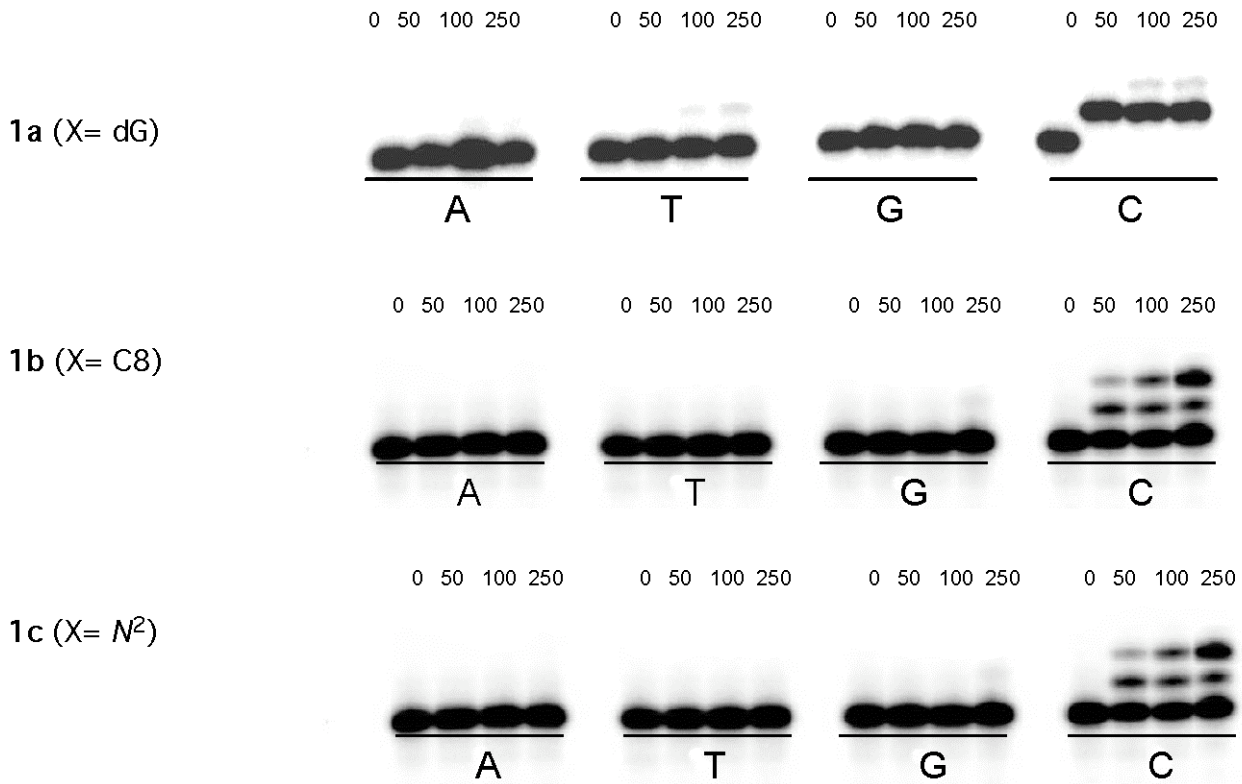


Figure S8. MALDI-TOF spectrum of oligonucleotide 2c.

3' -CCC CCG AGC ATT CCT AAC CX_C GGC TCA-5' (1)
 5' -³²P-GGG GGC TCG TAA GGA TTG G



3' -CCC CCG AGC ATT CCT AAC CGC GX_C TCA-5' (2)
 5' -³²P-GGG GGC TCG TAA GGA TTG GCG C

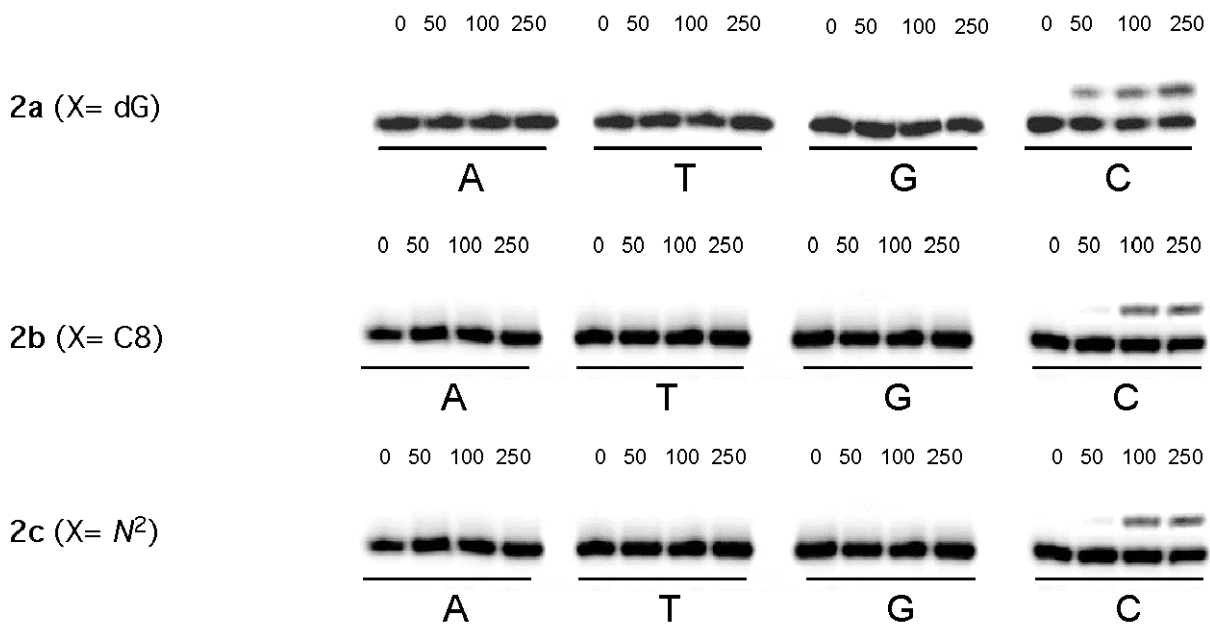
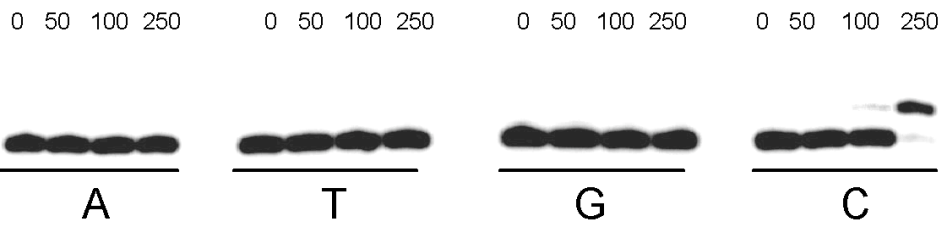


Figure S9. Single nucleotide incorporation of oligonucleotides **1a-c** and **2a-c** by Kf

3'-CCC CCG AGC ATT CCT AAC CXC GGC TCA-5' (**1b**)
 5'-³²P-GGG GGC TCG TAA GGA TTG G-- C



3'-CCC CCG AGC ATT CCT AAC CXC GGC TCA-5' (**1b**)
 5'-³²P-GGG GGC TCG TAA GGA TTG G-- CC

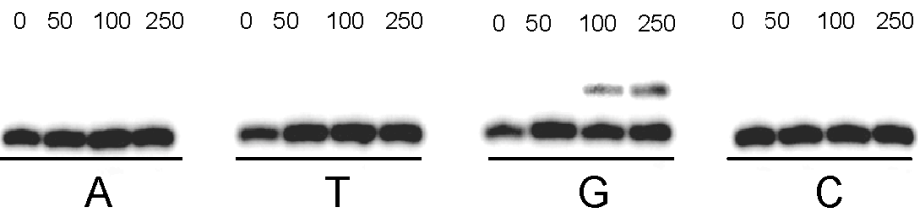
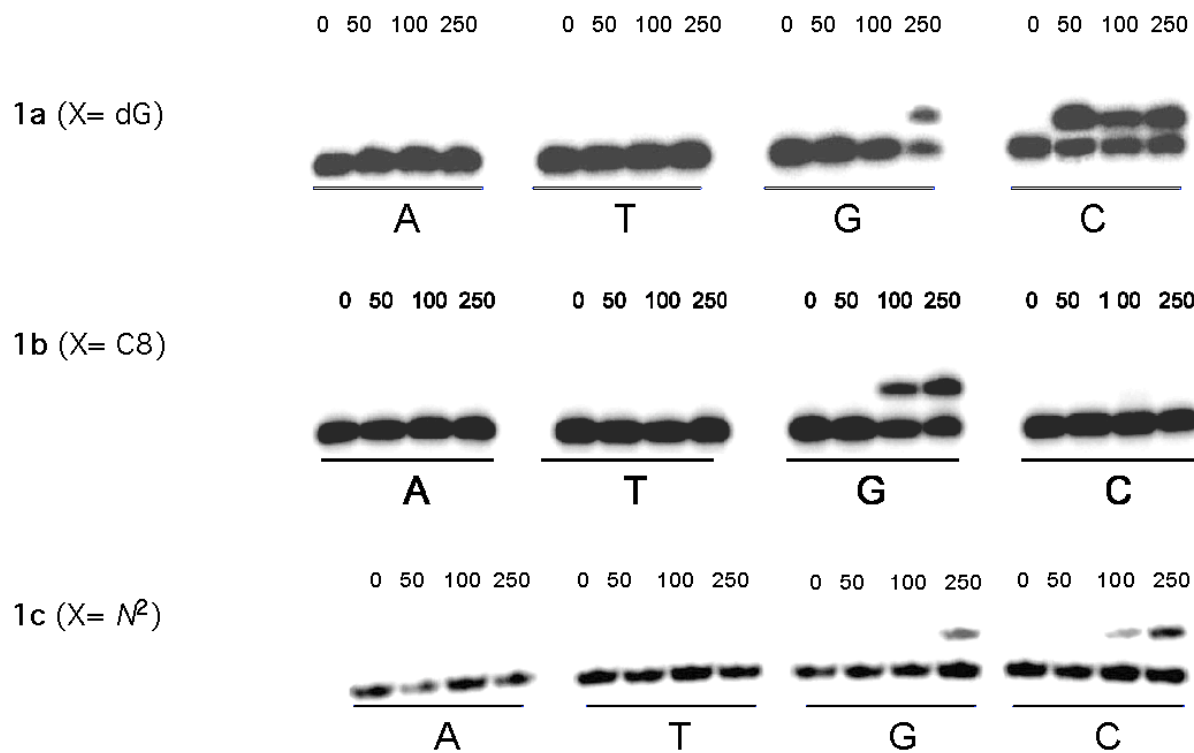


Figure S10. Single nucleotide incorporation of oligonucleotides **1b** with a 0- and +1 primers.

3'-CCC CCG AGC ATT CCT AAC CX_C GGC TCA-5' (1)
 5'-³²P-GGG GGC TCG TAA GGA TTG G



3'-CCC CCG AGC ATT CCT AAC CGC GX_C TCA-5' (2)
 5'-³²P-GGG GGC TCG TAA GGA TTG GCG C

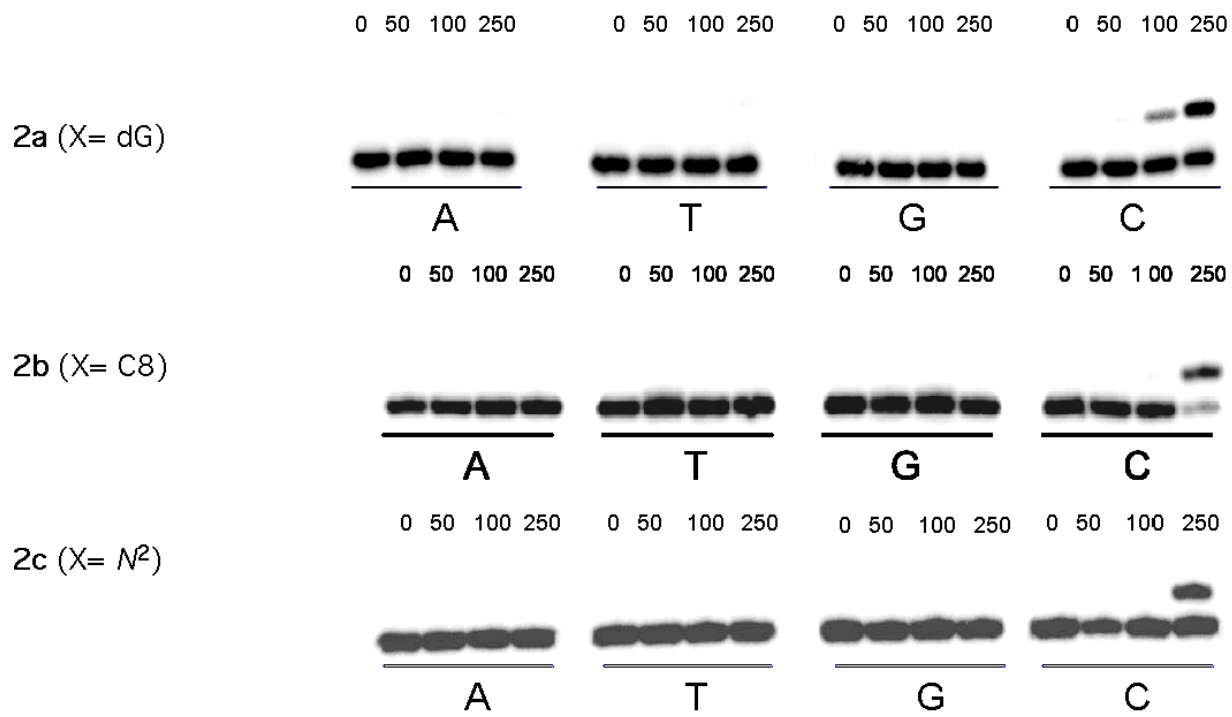


Figure S11. Single nucleotide incorporation of oligonucleotides **1a-c** and **2a-c** by pol II⁻

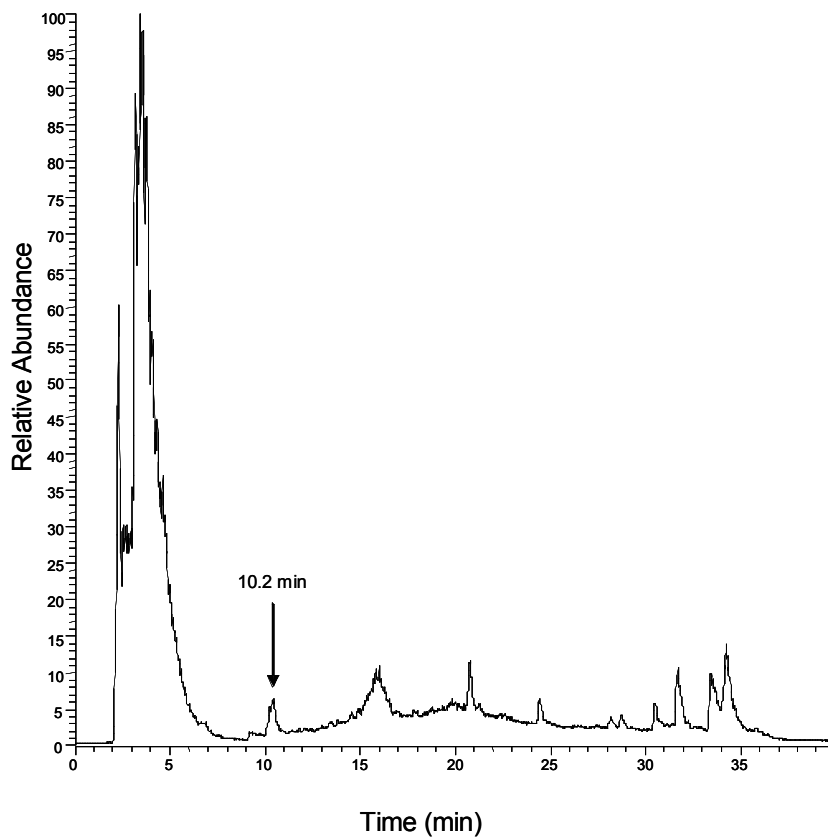


Figure S12. LC-ESI-MS/MS analysis of the pol II⁻ extension of oligonucleotide **1b**.

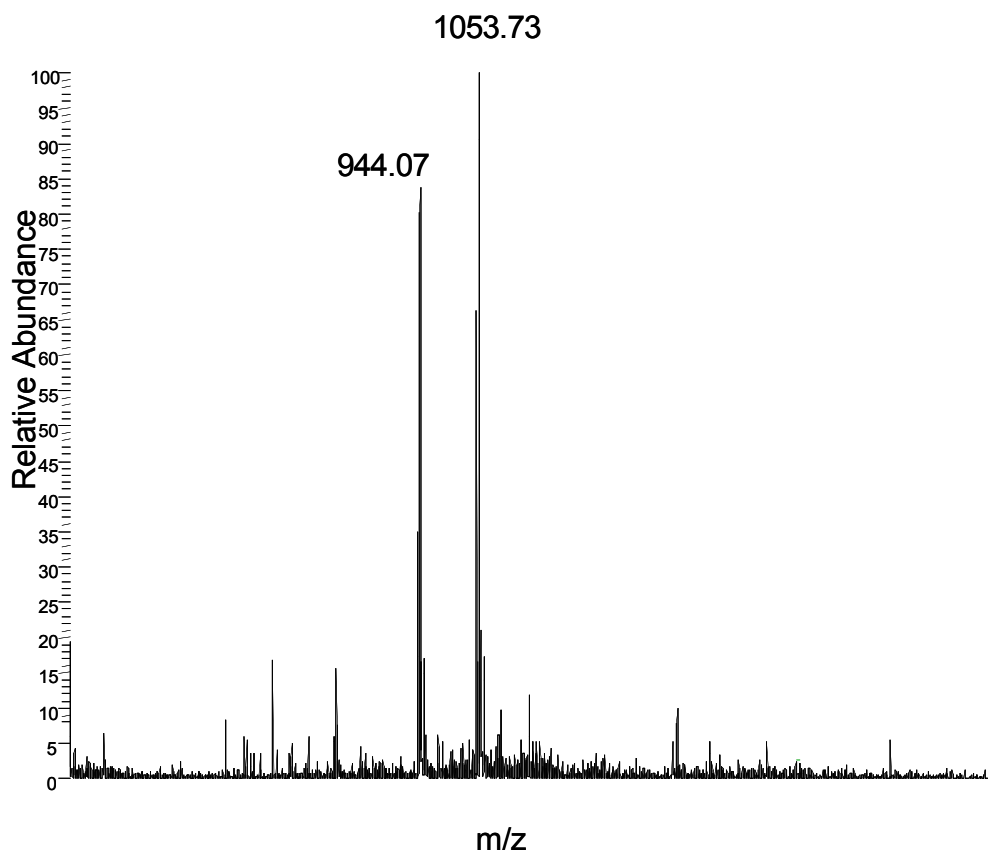


Figure S13. TIC spectrum of the pol II⁻ extension products from oligonucleotide **1b**.

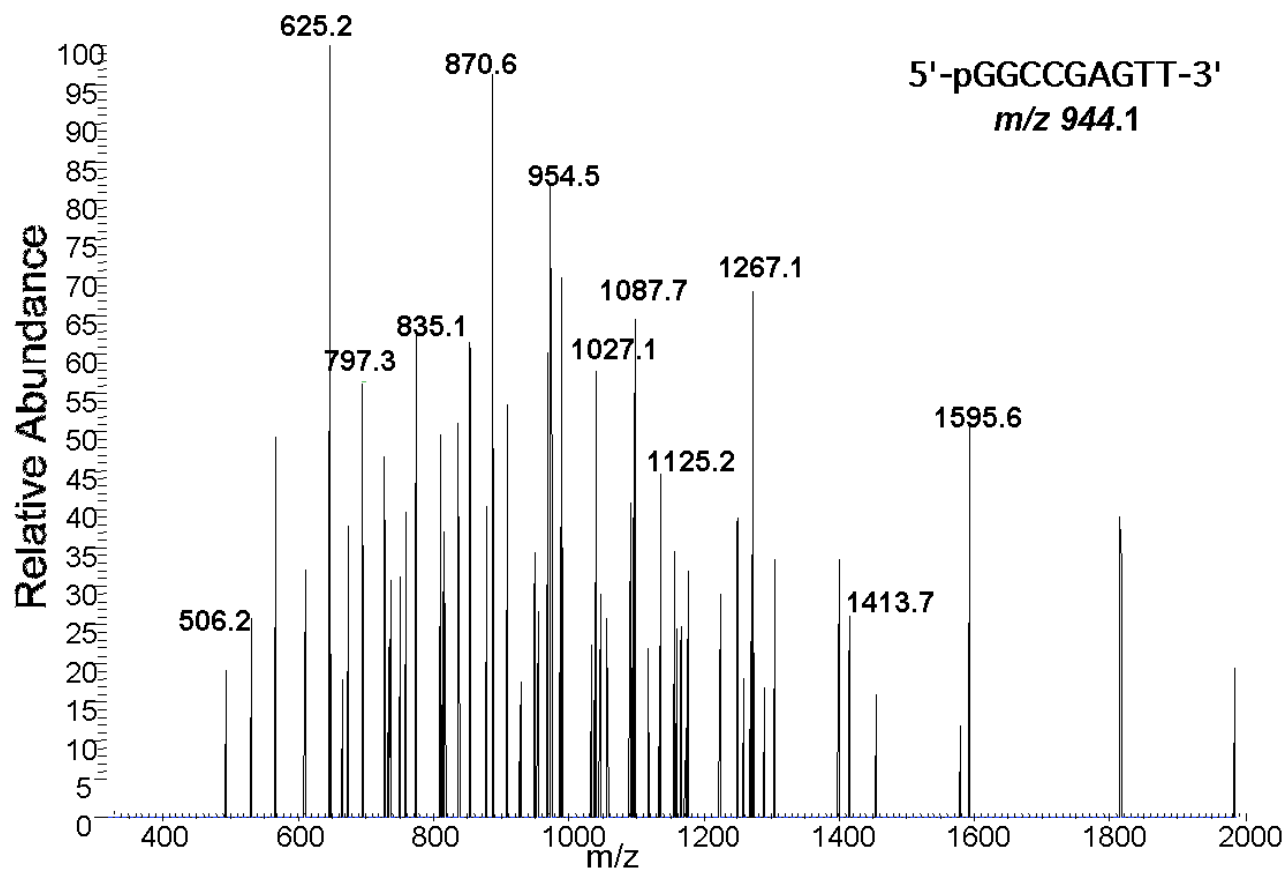


Figure S14. CID spectrum of the m/z 944.07 products from the pol II⁻ extension of oligonucleotide **1b**.

Table S1. Observed and calculated CID fragmentation of 5'-pGGCCGAGTT-3' (m/z 944.1)

Fragment assignment	observed	theoretical
5'-pG (a ₂ -B)	506.2	506.05
5'-pGG (a ₃ -B)	835.1	835.10
5'-pGGC (a ₄ -B)	1125.2	1124.14
5'-pGGCC (a ₅ -B)	1413.7	1413.19
5'-pGGCCG (a ₆ -B, -2)	870.7	870.62
5-pGGCCGA (a ₇ -B, -2)	1027.1	1027.15
pCCGAGT-3' (w ₇)	1087.7	1086.67
pGAGTT-3' (w ₅)	1595.6	1596.26
(w ₅ , -2)	797.4	797.62
pAGTT-3' (w ₄)	1267.1	1267.20
pGTT-3' (w ₃)	954.5	654.15
p-TT-3' (w ₂)	625.3	625.09

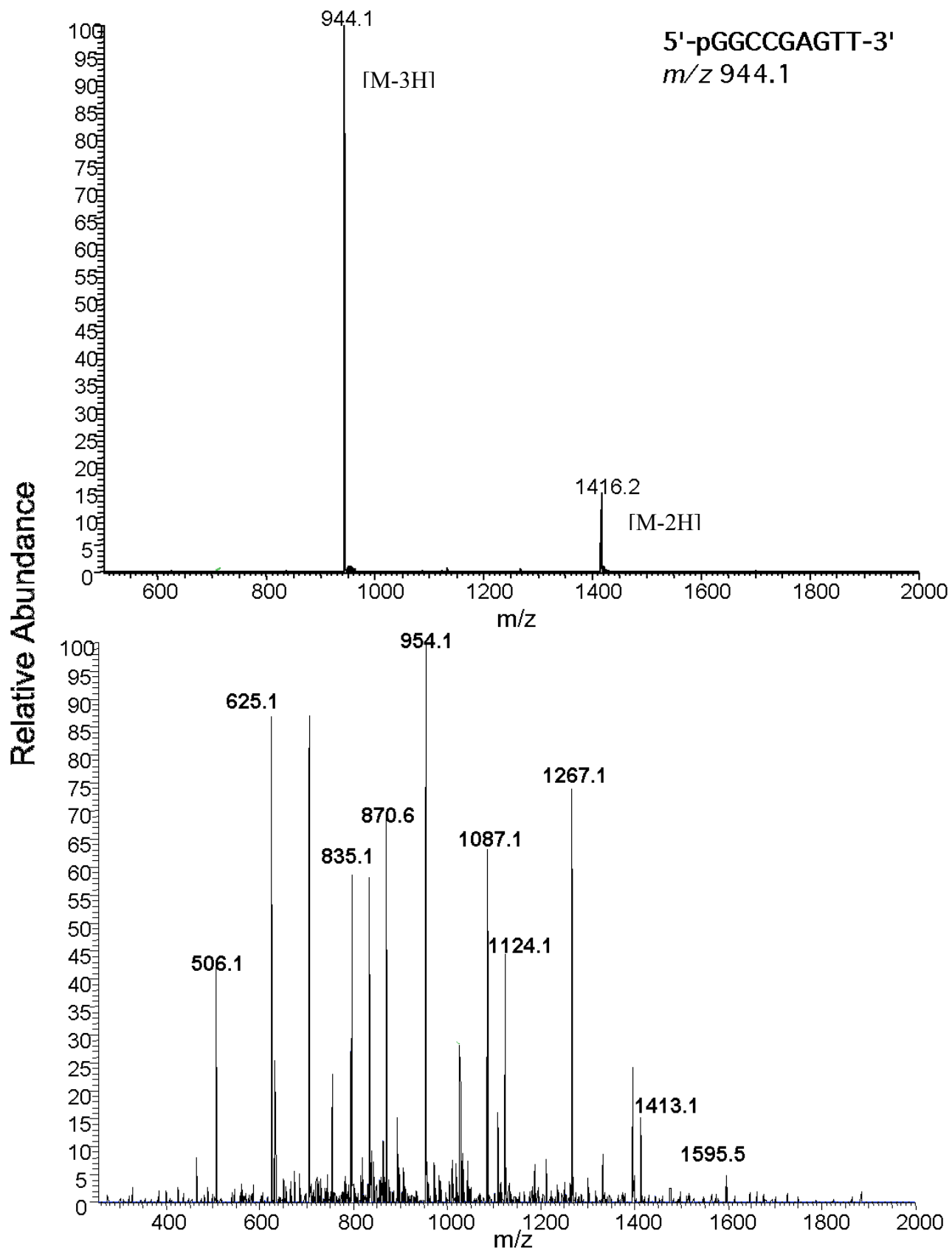


Figure S15. TIC (top) and CID (bottom) spectra of an authentic sample of 5'-pGGCCGAGTT-3' (*m/z* 944.1)

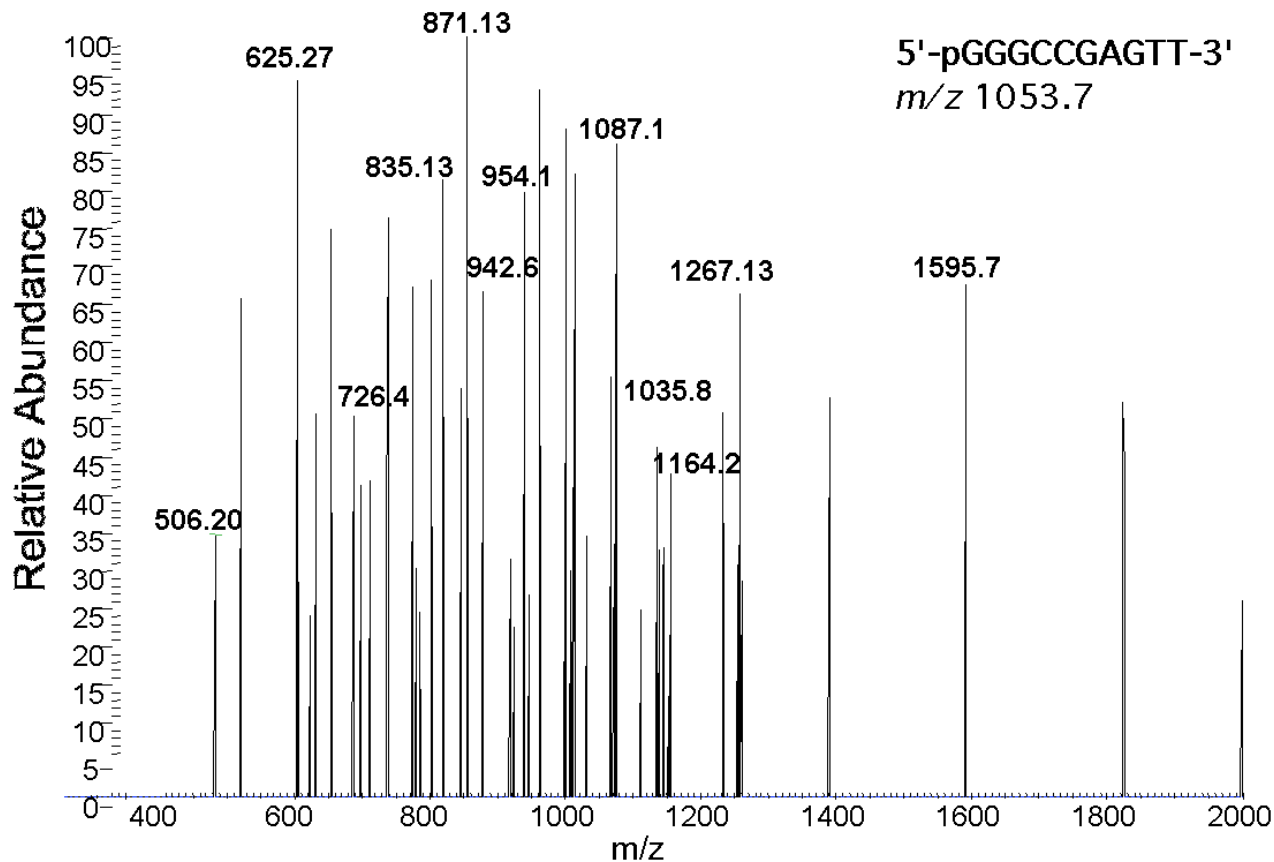


Figure S16. CID spectrum of the m/z 1053.7 products from the pol II⁻ extension of oligonucleotide **1b**.

Table S2. Observed and calculated CID fragmentation of 5'-pGGGCCGAGTT-3' (m/z 1053.7)

Fragment assignment	observed	theoretical
5'-pG (a ₂ -B)	506.2	506.05
5'-pGG (a ₃ -B)	835.1	835.10
5'-pGGG (a ₄ -B)	1164.2	1164.15
5'-pGGGC (a ₅ -B, -2)	726.4	726.09
5'-pGGGCC (a ₆ -B, -2)	871.13	870.62
5-pGGGCCG (a ₇ -B, -2)	1035.8	1035.14
pCCGAGTT-3' (w ₇ , -2)	1087.1	1086.67
pCCGAGTT-3' (w ₆ , -2)	942.6	942.15
pGAGTT-3' (w ₅)	1595.7	1596.26
pAGTT-3' (w ₄)	1267.1	1267.20
pGTT-3' (w ₃)	954.5	954.15
p-TT-3' (w ₂)	625.3	625.09

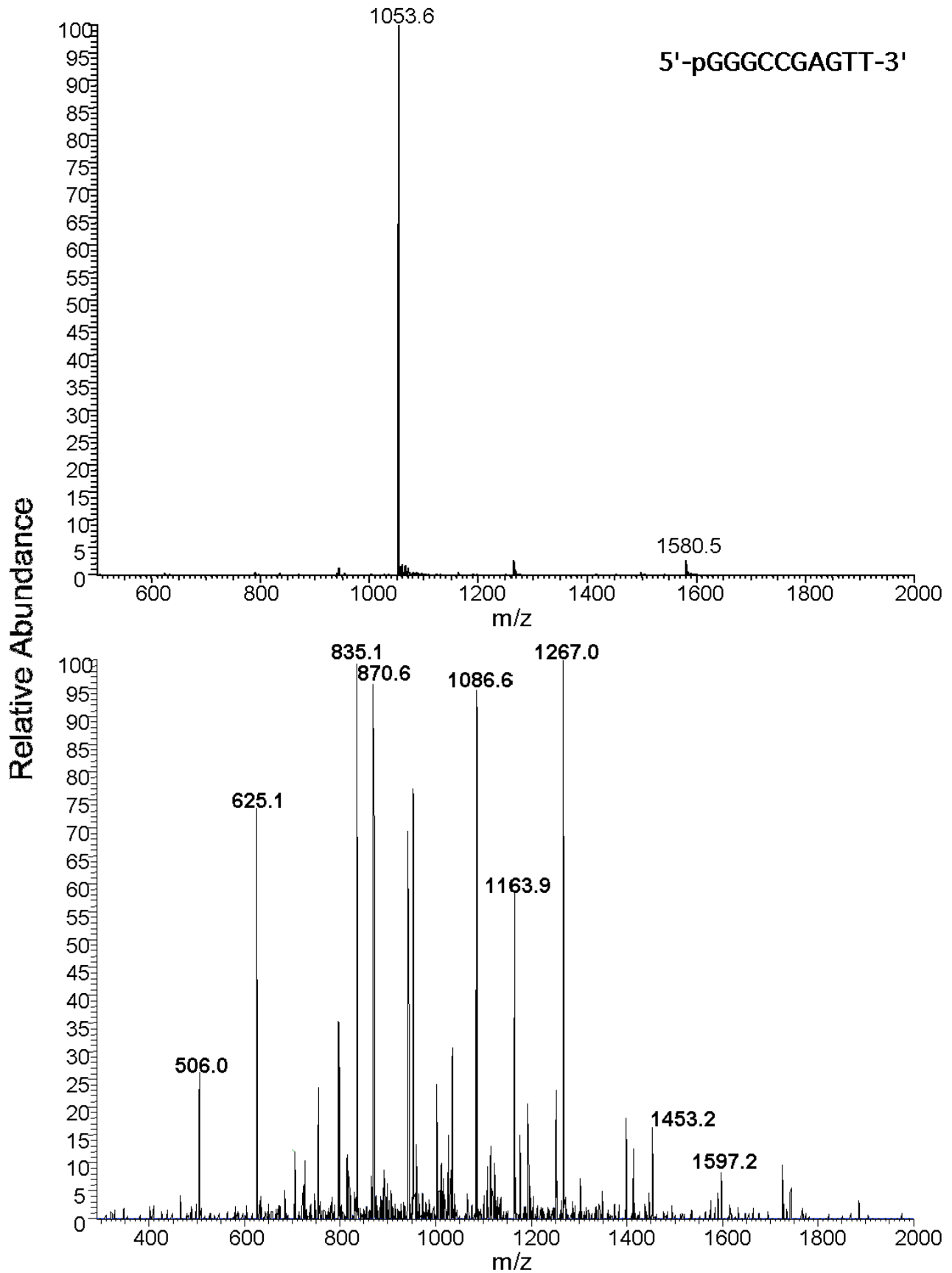


Figure S17. TIC (top) and CID (bottom) spectra of an authentic sample of 5'-pGGGCCGAGTT-3' (m/z 1053.7)

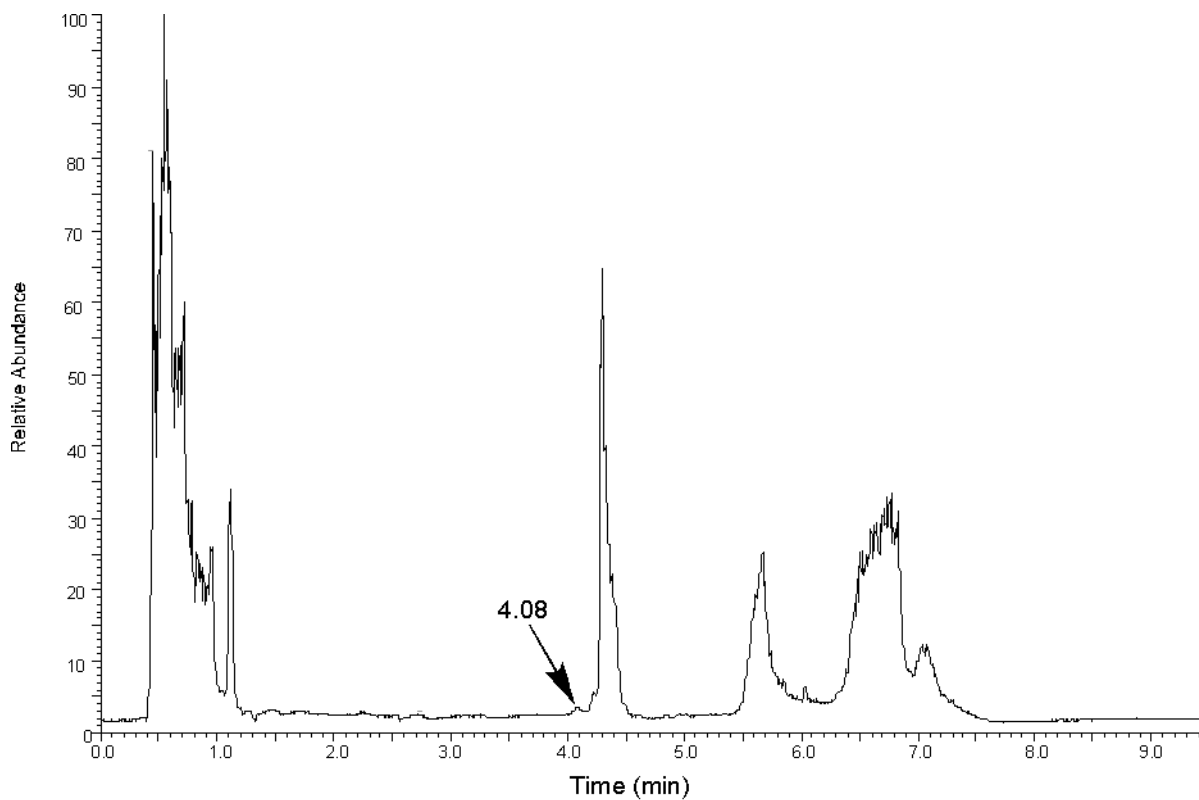


Figure S18. LC-ESI-MS/MS analysis of the pol II⁻ extension of oligonucleotide **2b**

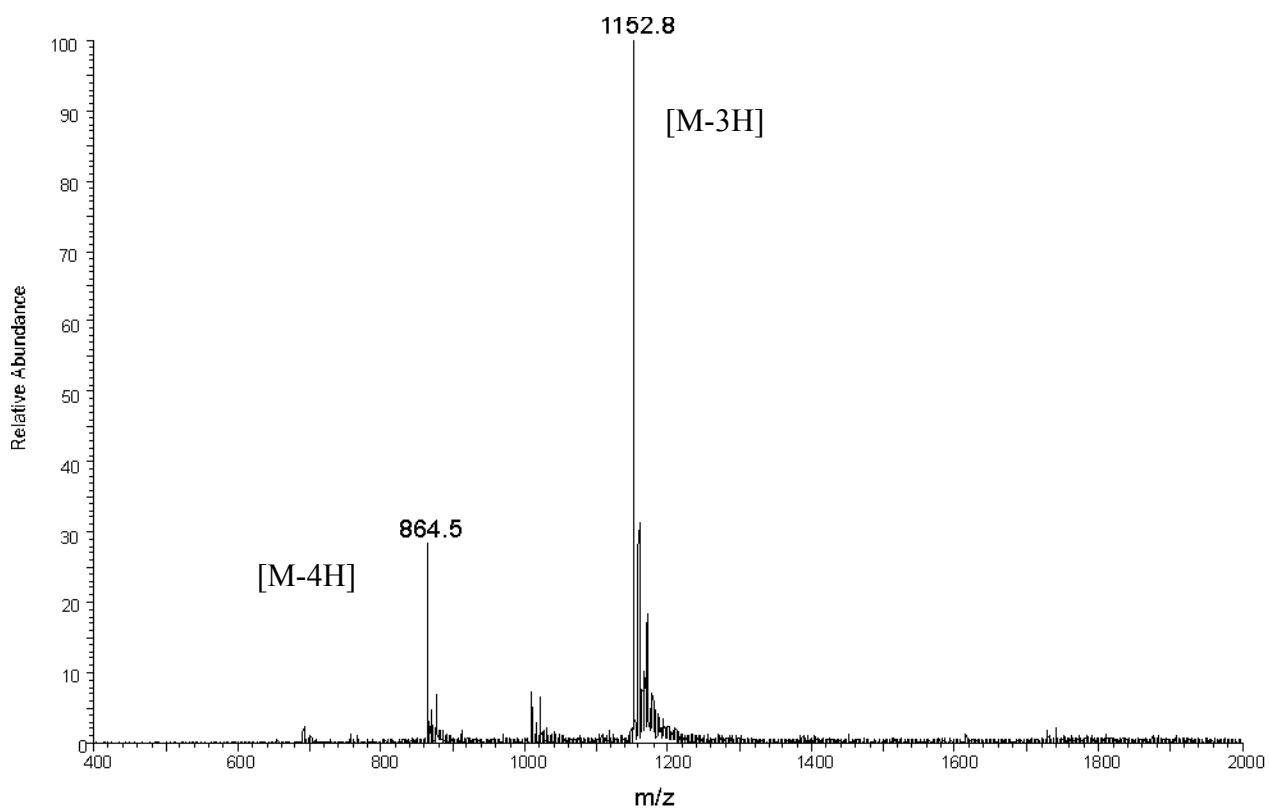


Figure S19. TIC spectrum of the pol II⁻ extension products from oligonucleotide **2b**

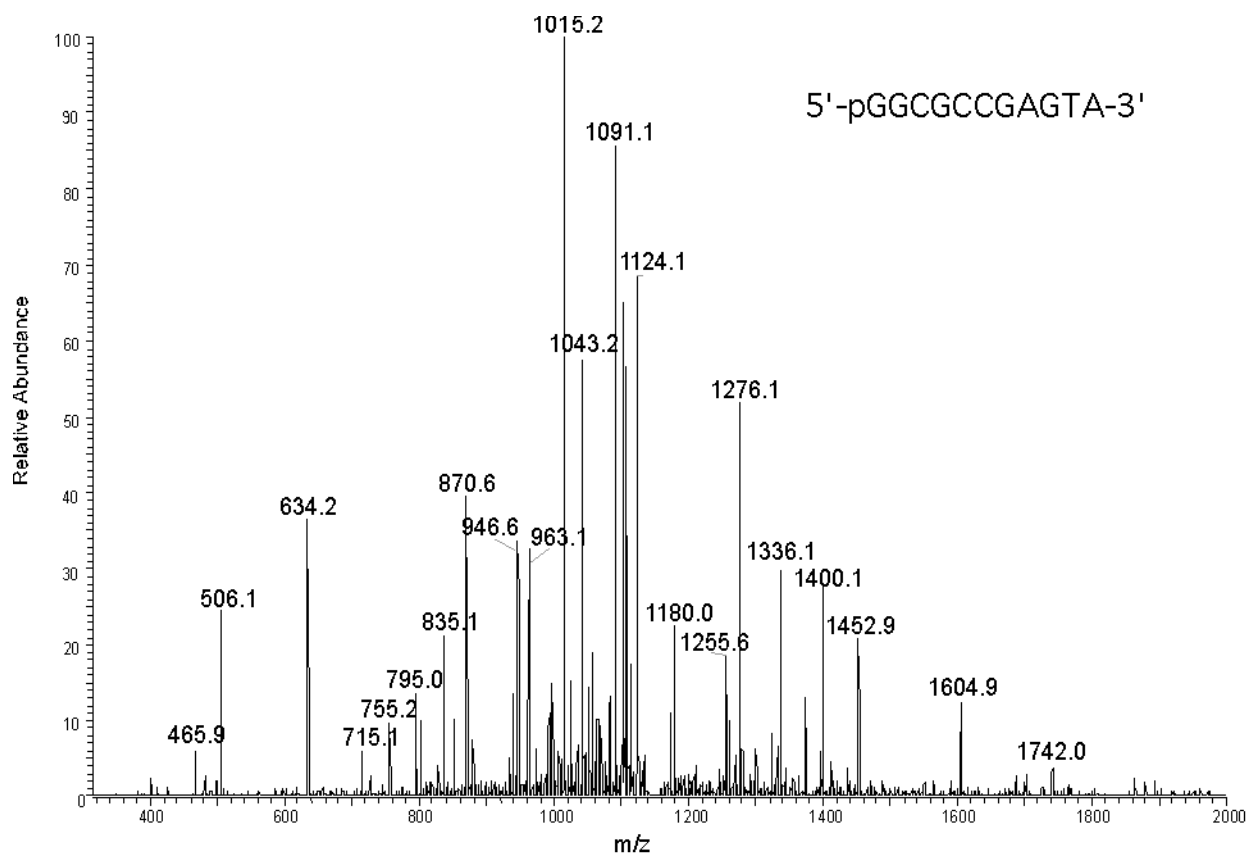


Figure S20. CID spectrum of the m/z 1152.8 products from the pol II⁻ extension of oligonucleotide **2b**.

Table S3. Observed and calculated CID fragmentation of 5'-pGGCGCCGAGTA-3' (m/z 1015.8)

Fragment assignment	observed	theoretical
5'-pG (a ₂ -B)	506.1	506.05
5'-pGG (a ₃ -B)	835.1	835.10
5'-pGGC (a ₄ -B)	1124.1	1124.14
5'-pGGCG (a ₅ -B)	1452.9	1453.20
5'-pGGCGC (a ₆ -B)	1742.0	1742.2
(a ₆ -B, -2)	870.6	870.62
5-pGGCGCC (a ₇ -B, -2)	1015.2	1015.14
5-pGGCGCCG (a ₈ -B, -2)	1180.0	1179.67
5-pGGCGCCG (a ₉ -B, -2)	1336.1	1336.20
pCGCCGAGTA-3' (w ₉ , -2)	1400.1	1400.22
pGCCGAGTA-3' (w ₈ , -2)	1255.9	1255.70
pCCGAGTA-3' (w ₇ , -2)	1091.2	1091.18
pCGAGTA-3' (w ₆ , -2)	946.6	946.65
pGAGTA-3' (w ₅)	1604.9	1605.27
pAGTA-3' (w ₄)	1276.1	1276.21
pGTA-3' (w ₃)	963.1	963.16
p-TA-3' (w ₂)	634.2	634.11

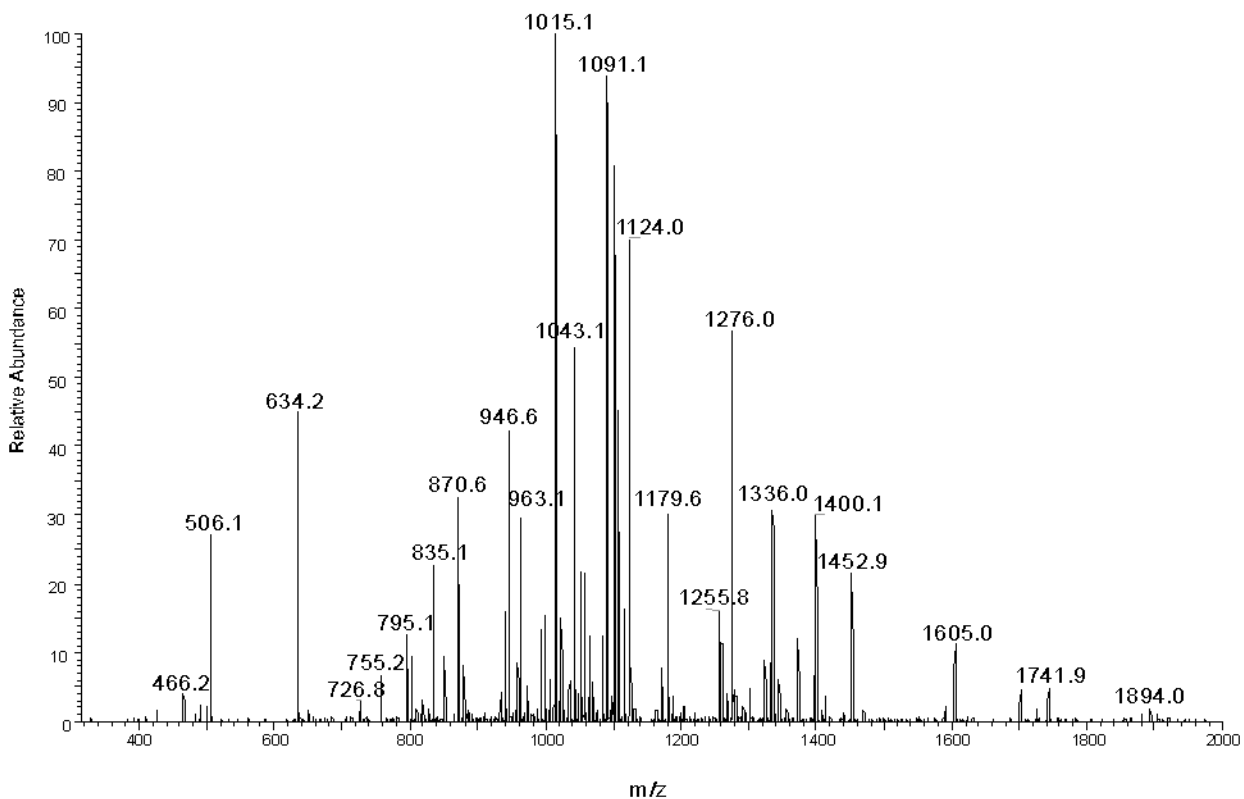
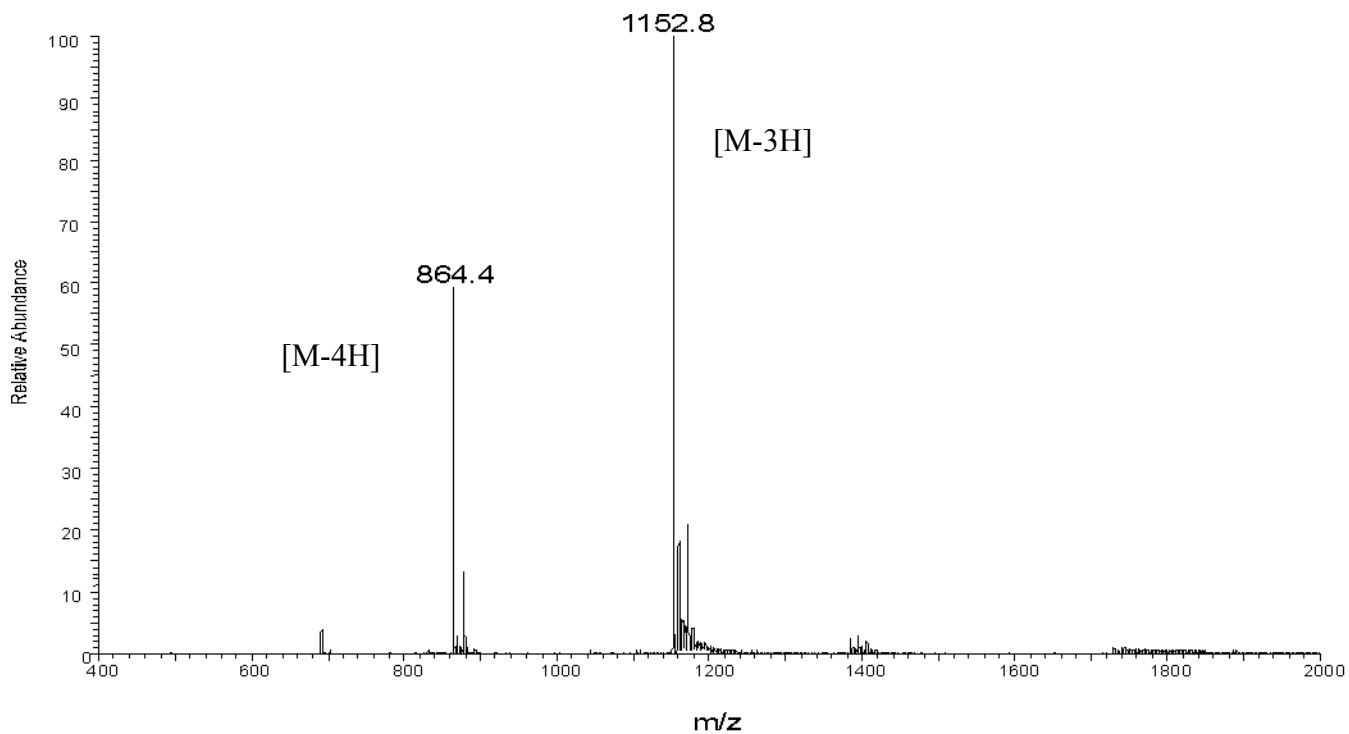


Figure S21. TIC (top) and CID (bottom) spectra of an authentic sample of 5'pGGCGCCGAGTA-3' (m/z 1052)

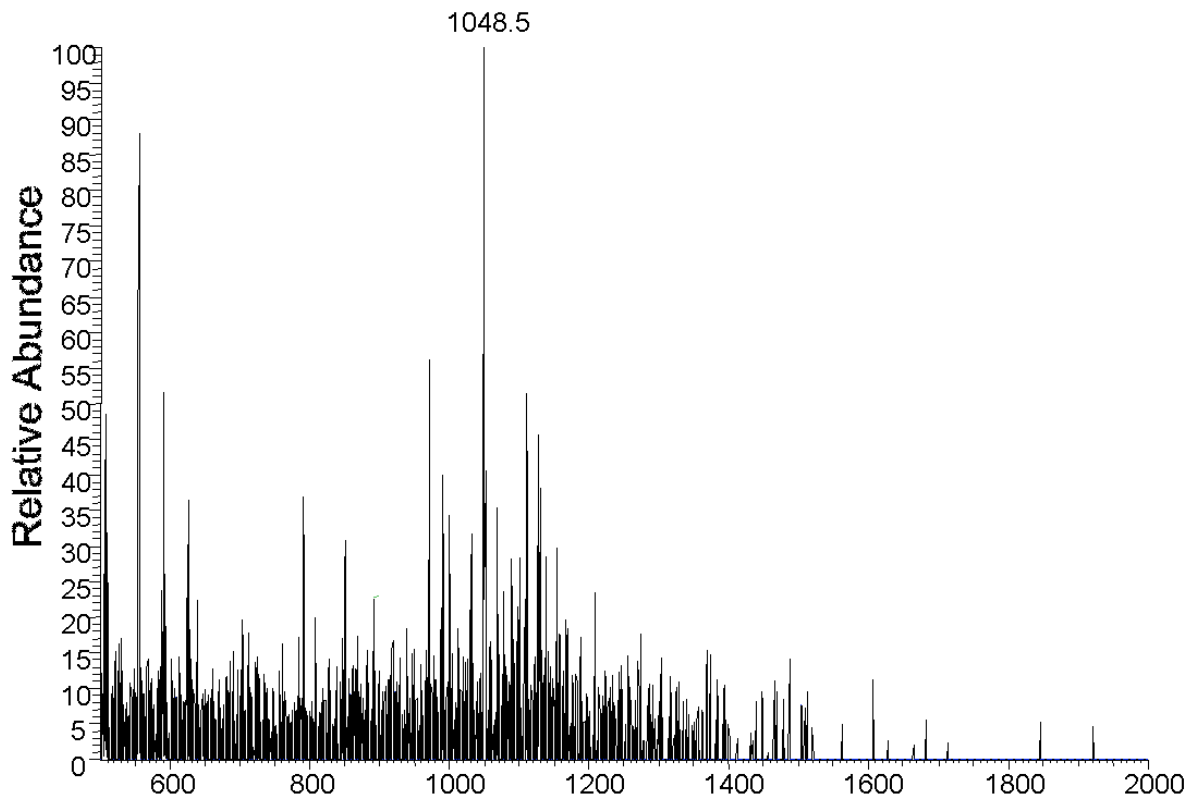


Figure S22. TIC spectrum of the pol II⁻ extension of oligonucleotide **2c**

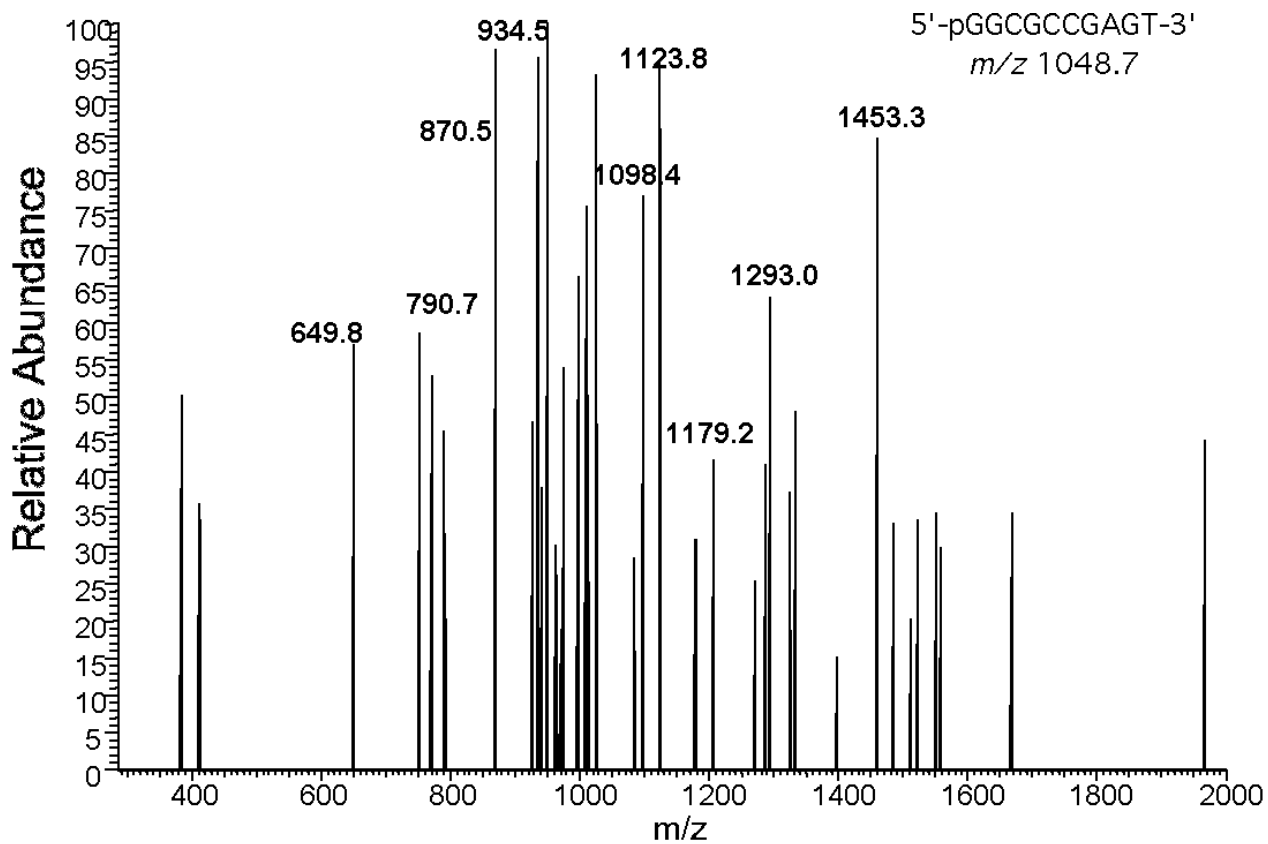


Figure S23. CID spectrum of the m/z 1048.7 product from the pol II⁻ extension of oligonucleotide **2c**.

Table S4. Observed and calculated CID fragmentation of 5'-pGGCGCCGAGT-3'; m/z 1048.7 (M-3H)

Fragment assignment	observed	theoretical
5'-pGGC (a_4 -B)	1124.0	1124.14
5'-pGGCG (a_5 -B)	1453.0	1453.20
5'-pGGCGC (a_6 -B, -2)	870.5	870.62
5'-pGGCGCCG (a_8 -B, -2)	1179.2	1179.67
pGCCGAGT-3' (w_7 , -2)	1098.4	1099.17
pCCGAGT-3' (w_6 , -2)	934.5	934.65
pCGAGT-3' (w_5 , -2)	790.7	790.12
pGAGT-3' (w_4)	1293.0	1292.21
pAGT-3' (w_3)	963.2	963.16
pGT-3' (w_2)	649.8	650.10

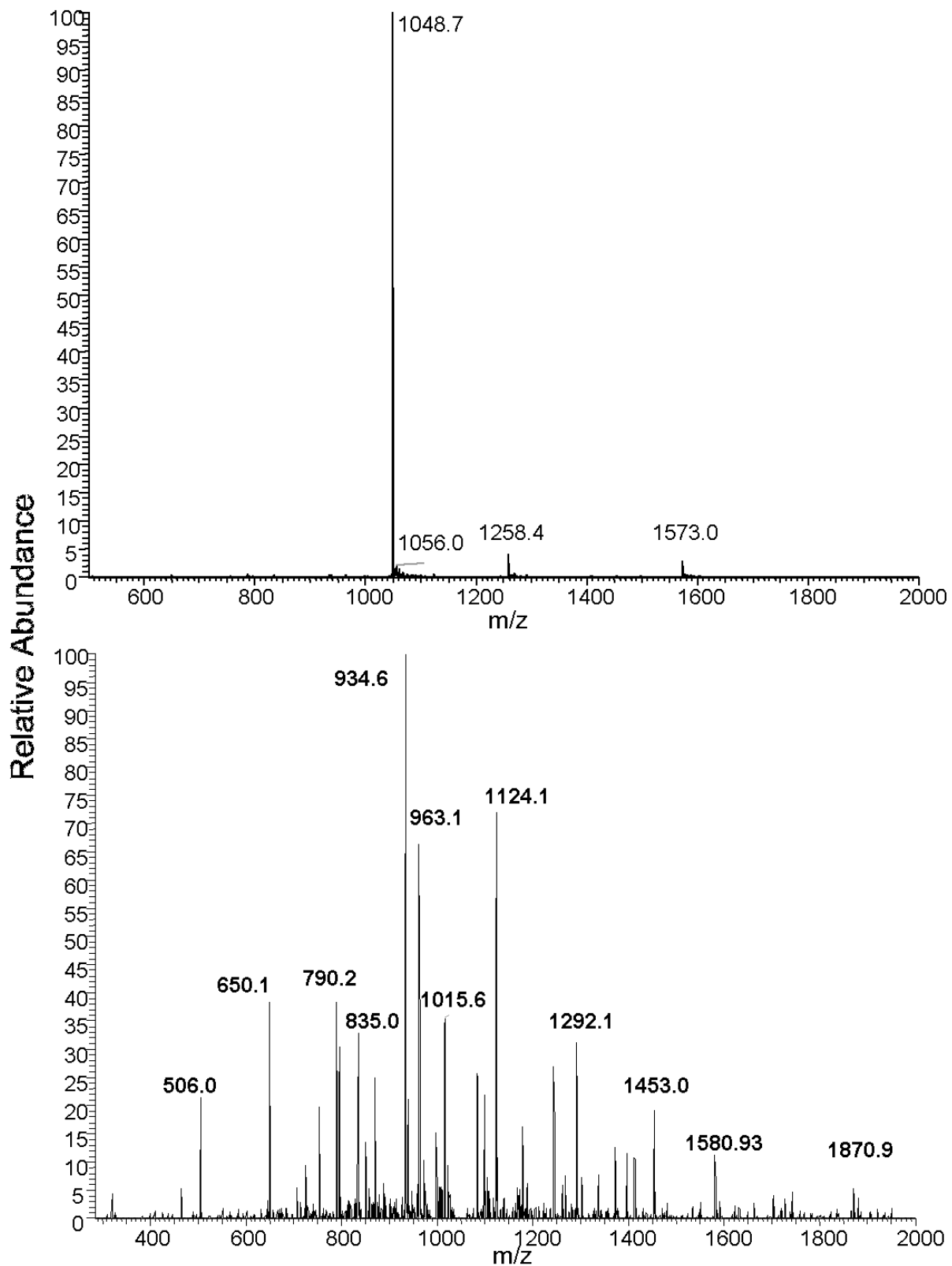
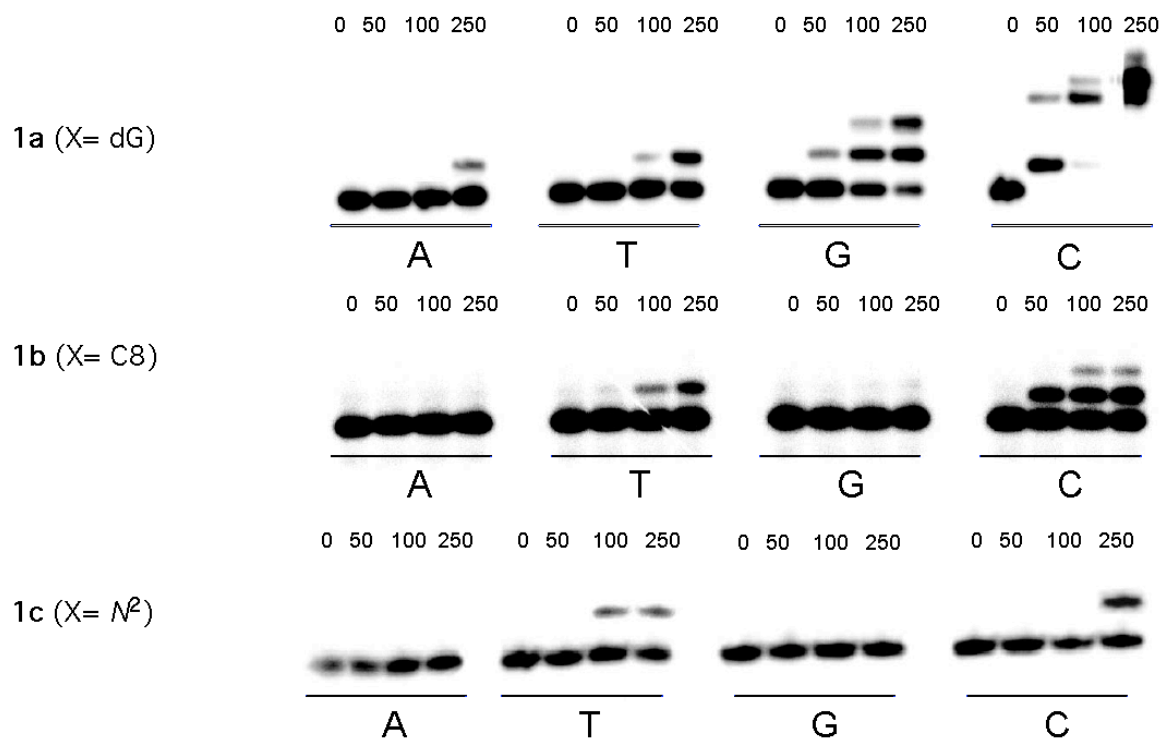


Figure S24. TIC (top) and CID (bottom) spectra of an authentic sample of 5'pGGCGCCGAGT-3' (m/z 1048.7)

3'-CCC CCG AGC ATT CCT AAC CX~~C~~ GGC TCA-5' (1)
 5'-³²P-GGG GGC TCG TAA GGA TTG G



3'-CCC CCG AGC ATT CCT AAC CGC GX~~C~~ TCA-5' (2)
 5'-³²P-GGG GGC TCG TAA GGA TTG GCG C

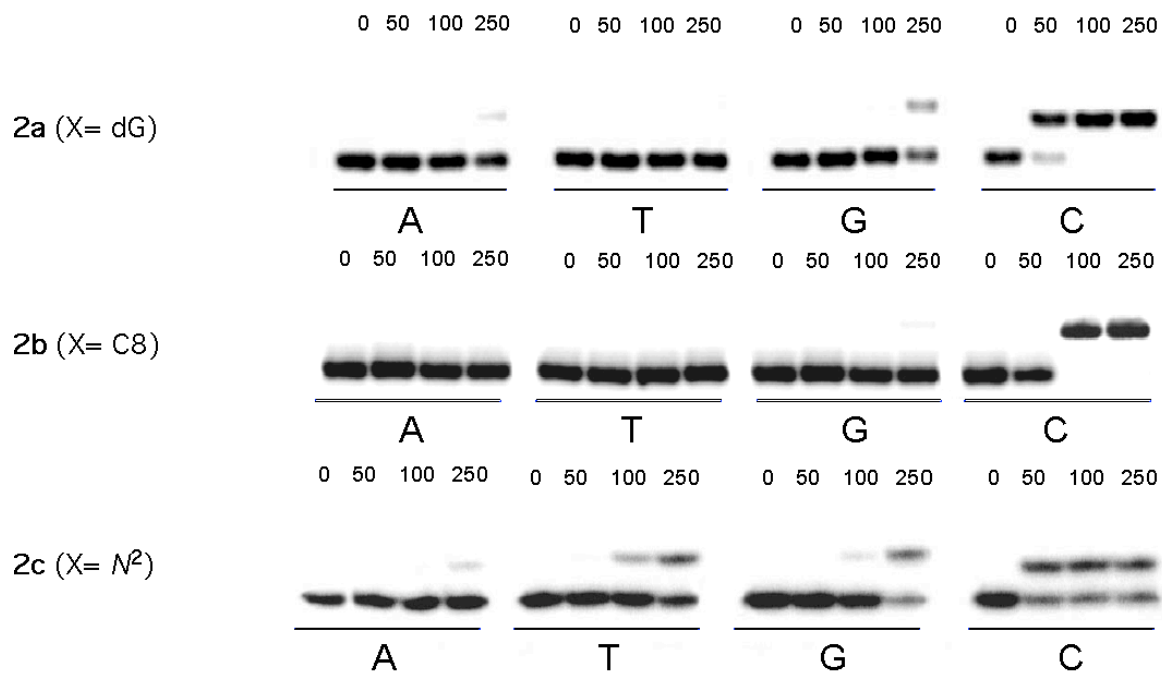


Figure S25. Single nucleotide incorporation of oligonucleotides **1a-c** and **2a-c** by Dpo4

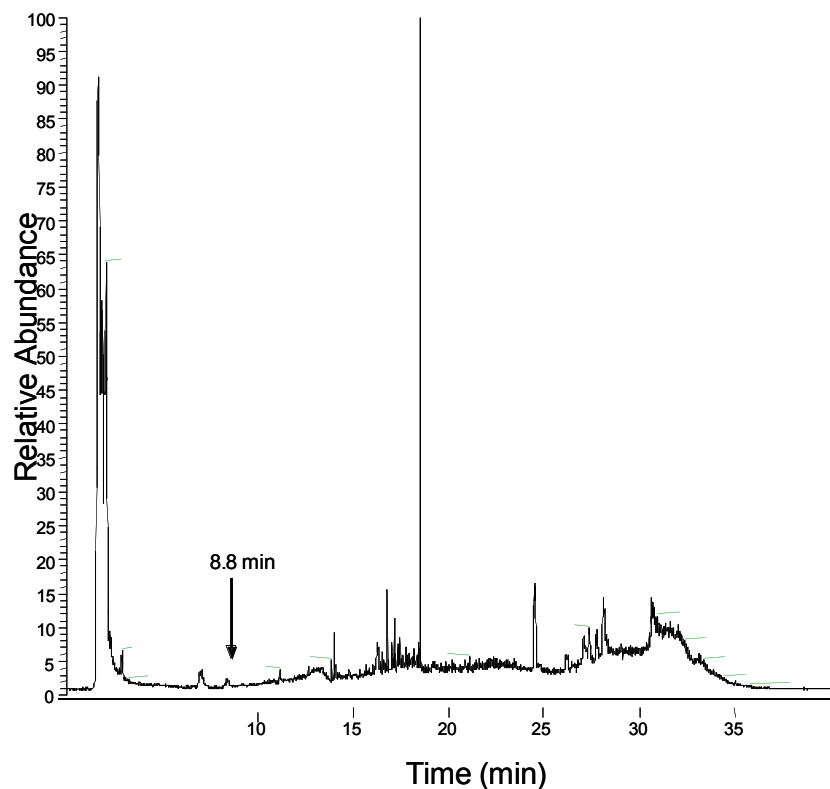


Figure S26. LC-ESI-MS/MS analysis of the Dpo4 extension of oligonucleotide **1b**.

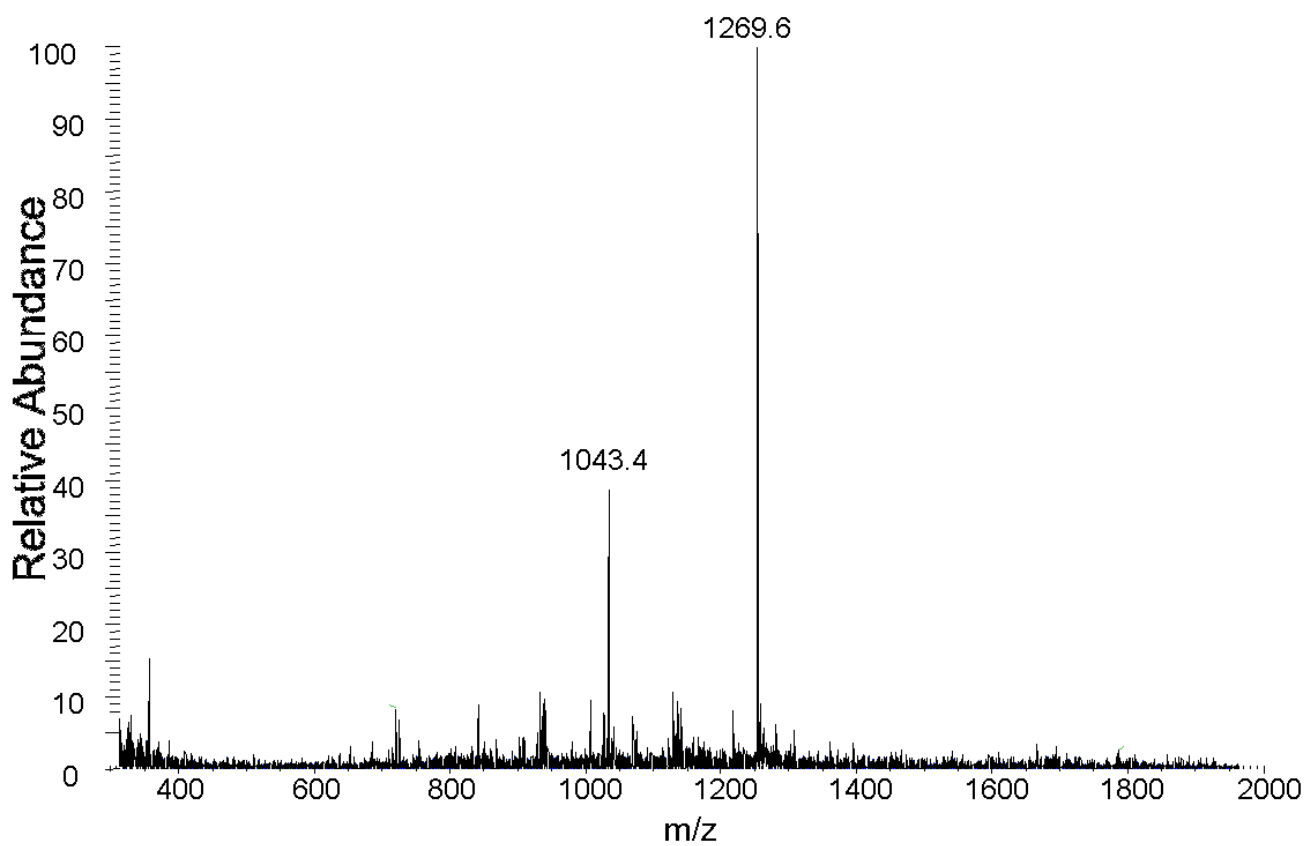


Figure S27. TIC spectrum of the Dpo4 extension products from oligonucleotide **1b**. The m/z 1269.6 is from the 5'-end of the primer (5'-GGGGCTCGTAAGGATp-3')

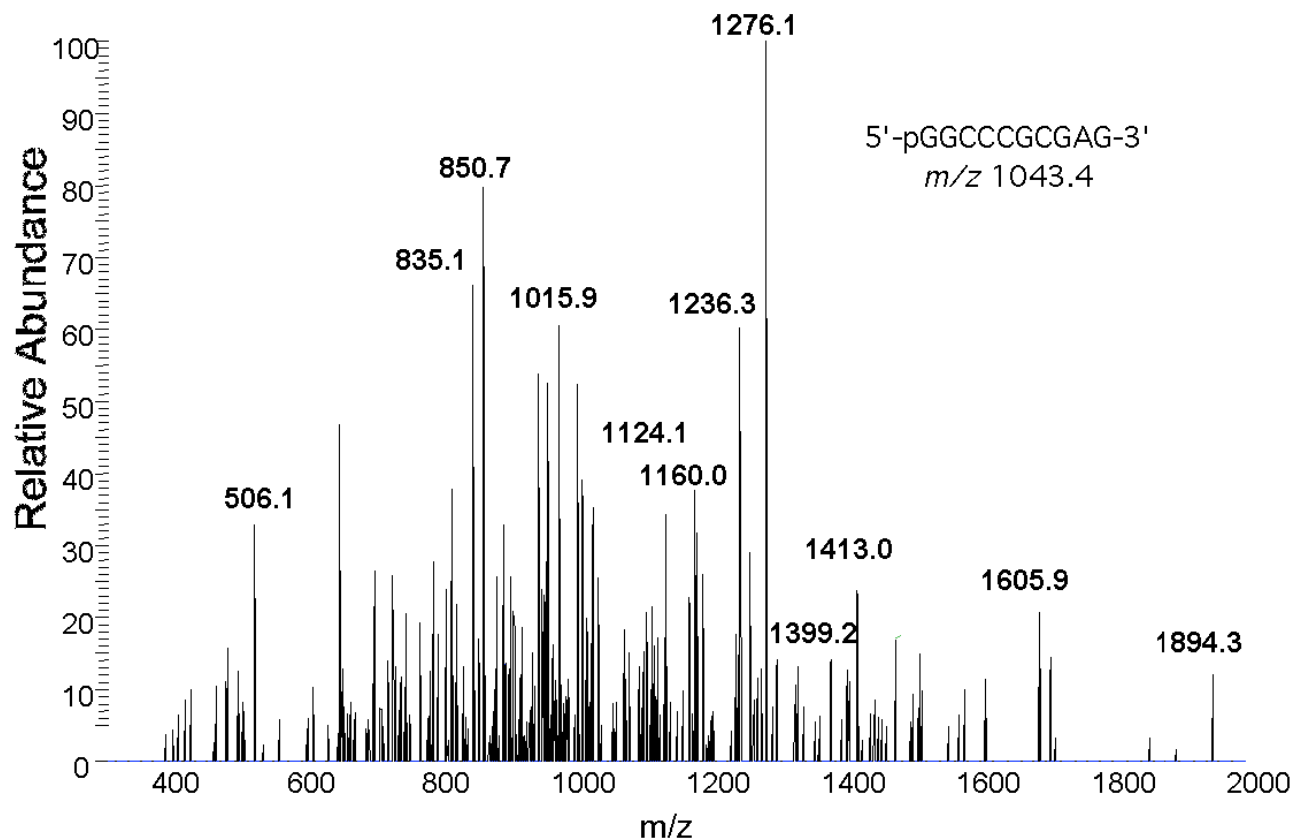


Figure S28. CID spectrum of the m/z 1043.4 product from the Dpo4 extension of oligonucleotide **1b**.

Table S5. Observed and calculated CID fragmentation of 5'-pGGCCCGCGAG-3'; m/z 1043.4 (M-3H)

Fragment assignment	observed	theoretical
5'-pG (a ₂ -B)	506.1	506.05
5'-pGG (a ₃ -B)	835.1	835.10
5'-pGGC (a ₄ -B)	1124.1	1124.14
5'-pGGCC (a ₅ -B)	1413.1	1413.19
5'-pGGCCC (a ₆ -B, -2)	850.7	850.61
5'-pGGCCCG (a ₇ -B, -2)	1015.9	1015.1
5'-pGGCCCGC (a ₈ -B, -2)	1160.0	1159.7
pGCCCGCGAG-3' (w ₉ , -2)	1399.2	1400.72
pCCCGCGAG-3' (w ₈ , -2)	1236.3	1236.20
pCGCGAG-3' (w ₆)	1985.3	1895.31
pGCGAG-3' (w ₄)	1605.9	1606.26
pCGAG-3' (w ₄)	1276.1	1277.21

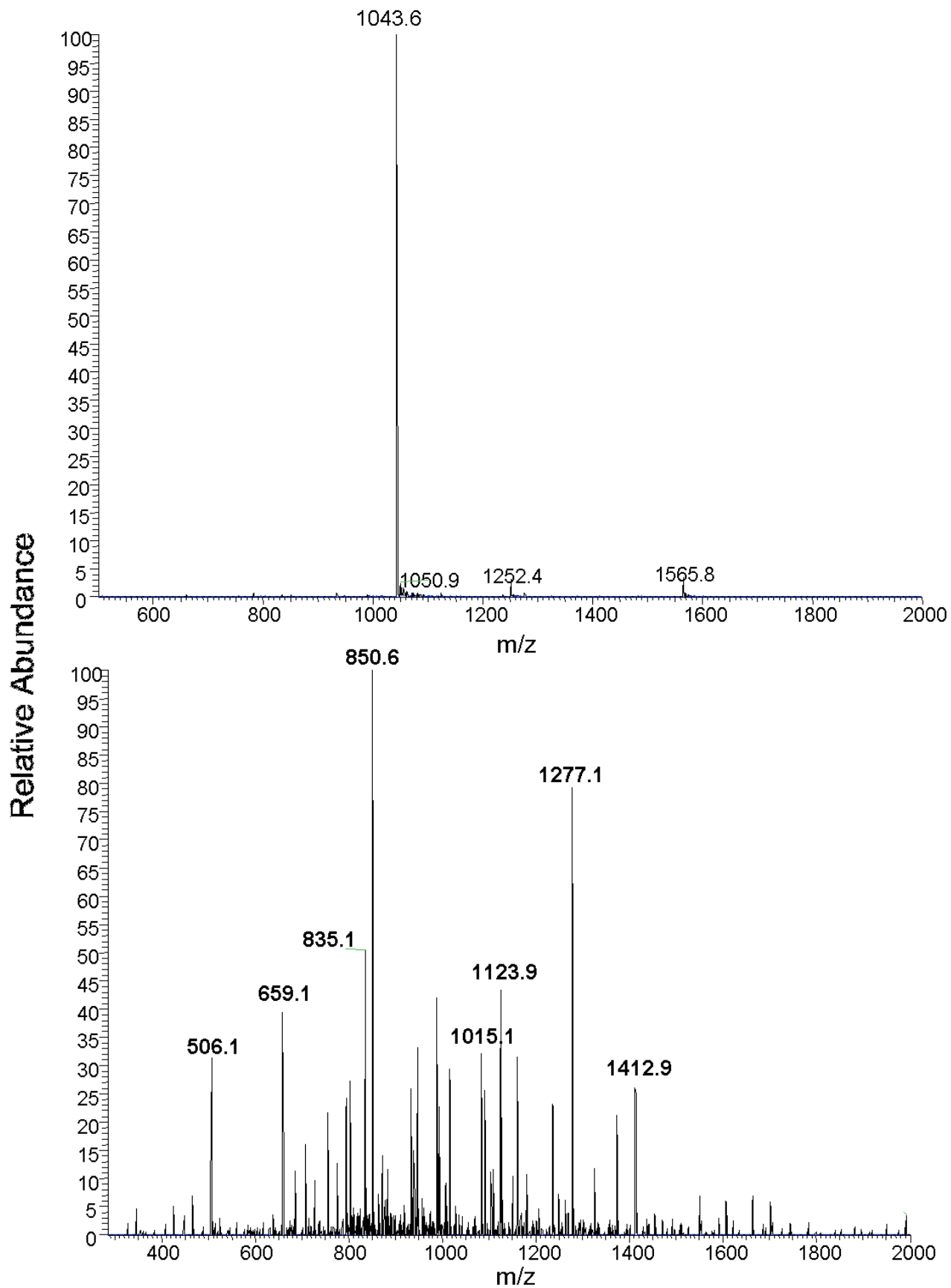


Figure S29. TIC (top) and CID (bottom) spectra of an authentic sample of 5'-pGGCCCGCGAG-3'; m/z 1043.4 (M-3H)

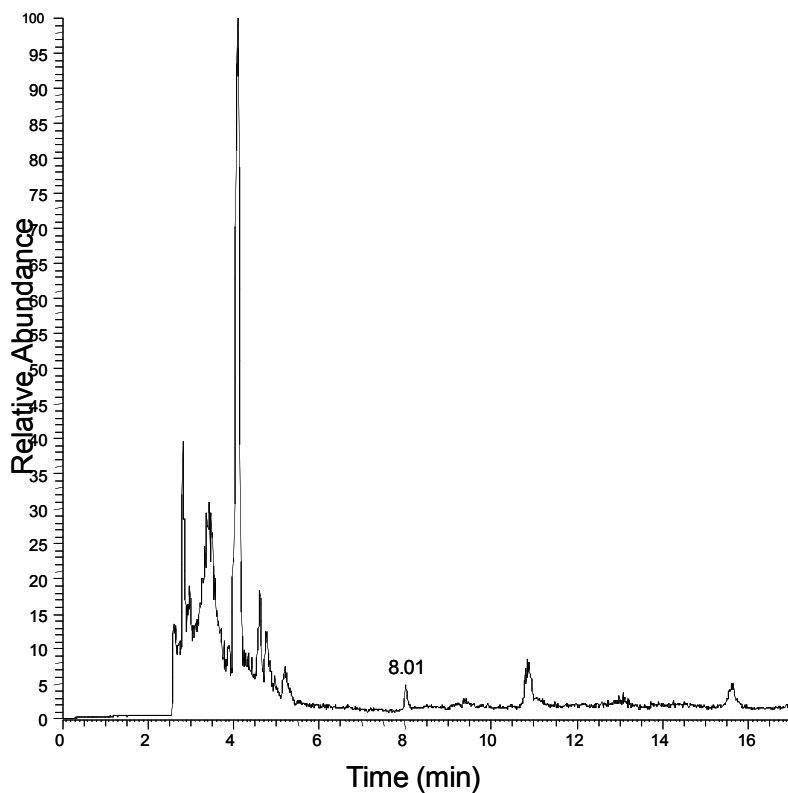


Figure S30. LC-ESI-MS/MS analysis of the Dpo4 extension of oligonucleotide **2b**

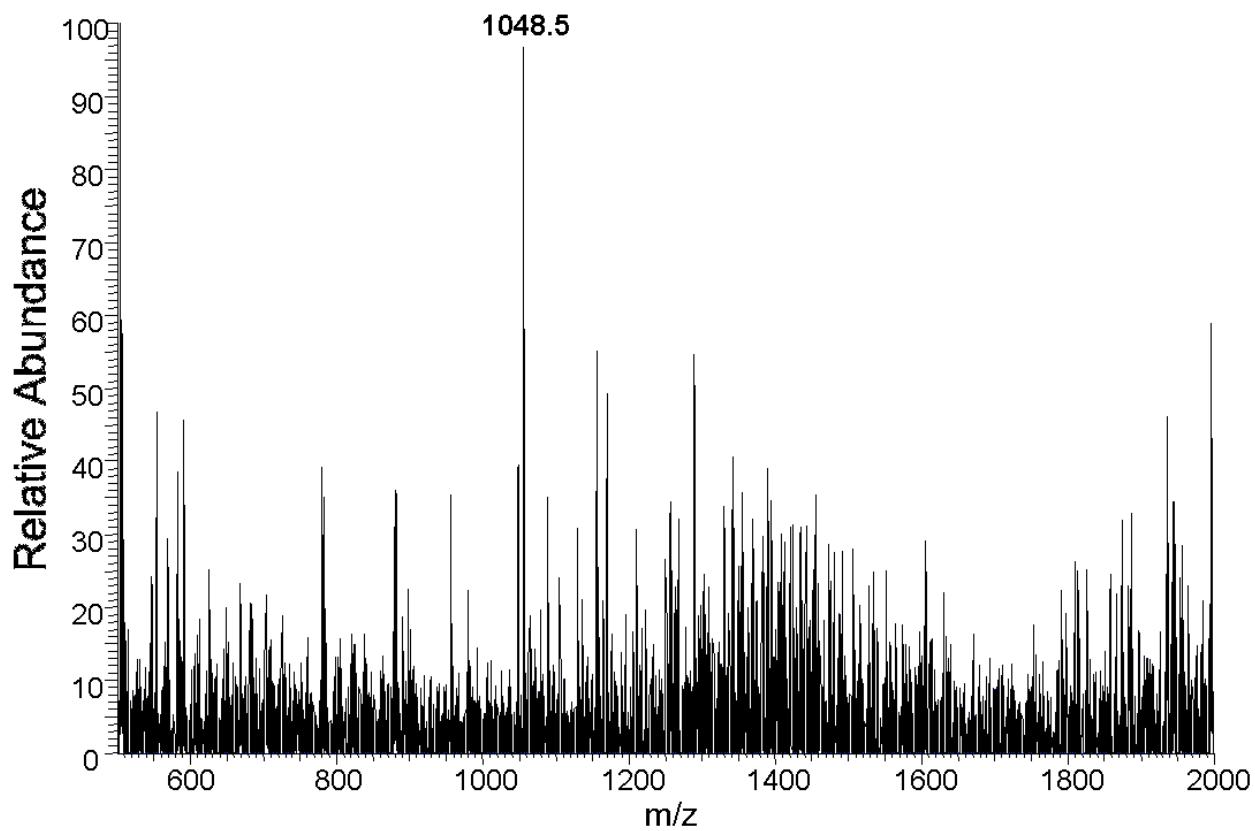


Figure S31. TIC spectrum of the Dpo4 extension products from oligonucleotide **2b**.

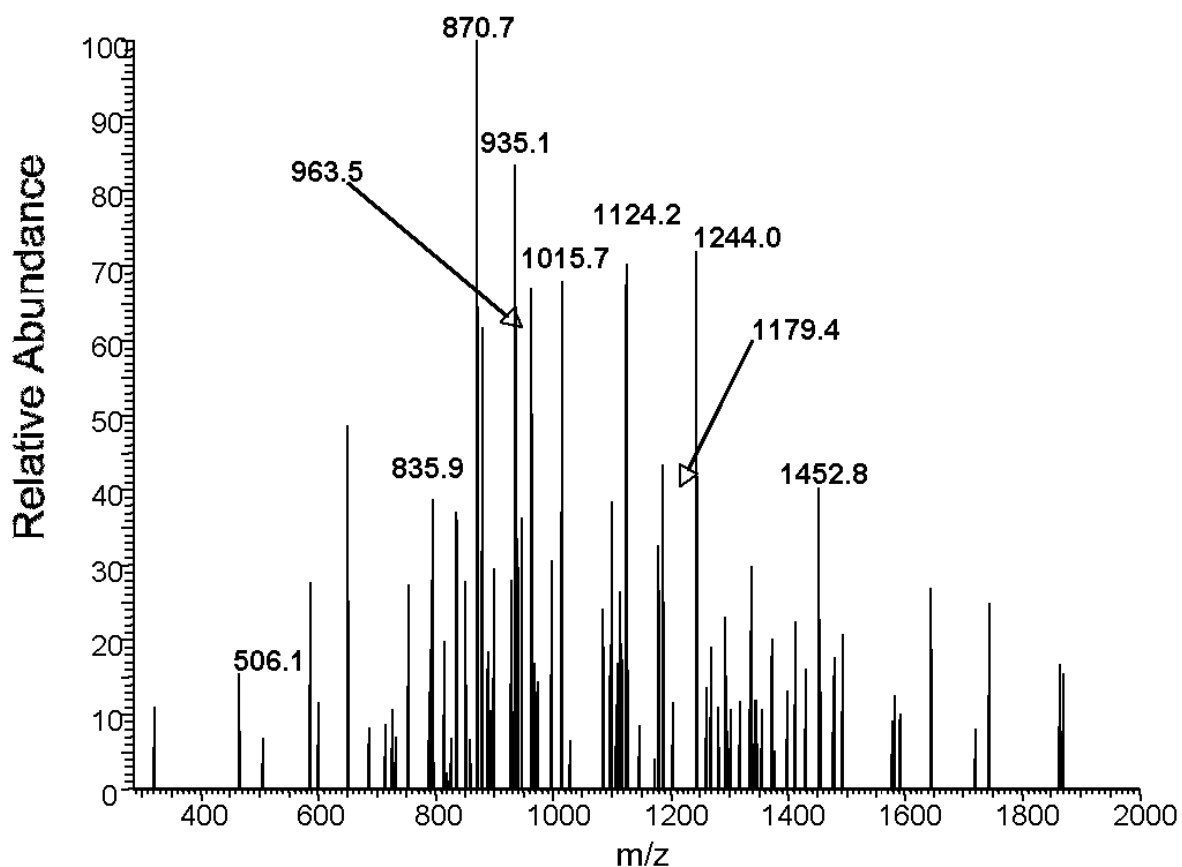
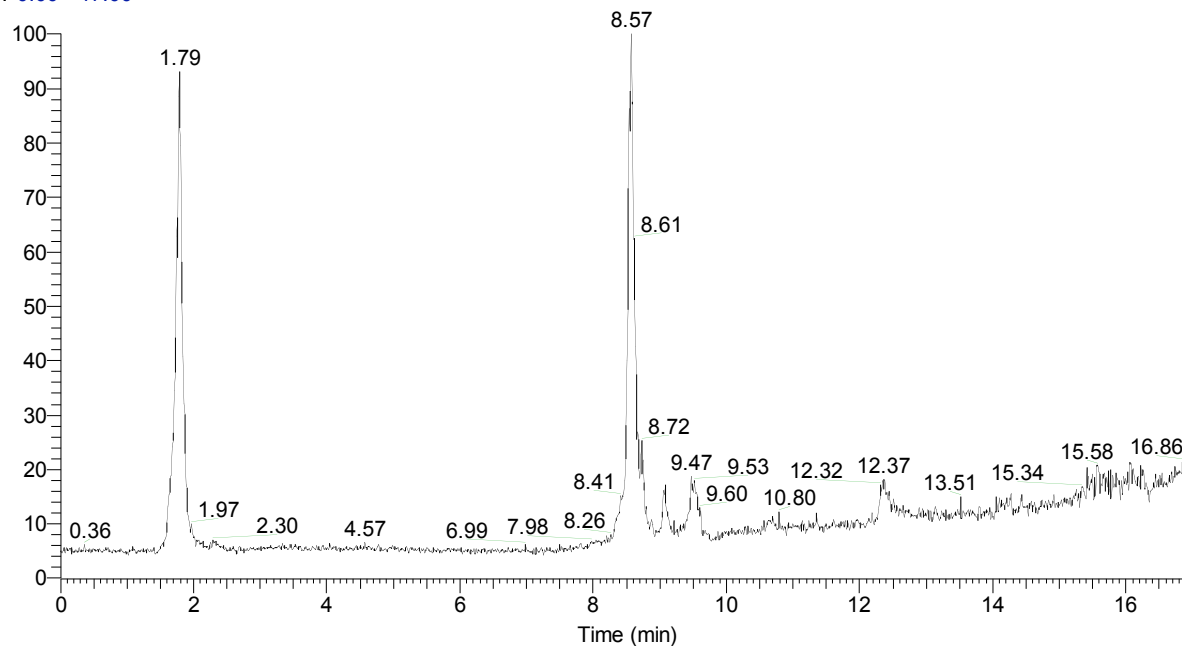


Figure S32. CID spectrum of the m/z 1048.5 products from the Dpo4 extension of oligonucleotide **2b**.

Table S6. Observed and calculated CID fragmentation of 5'-pGGCGCCGAGT-3' (m/z 1048.5)

Fragment assignment	observed	theoretical
5'-pG (a ₂ -B)	506.1	506.05
5-pGG (a ₃ -B)	835.9	835.10
5'-pGGC (a ₄ -B)	1124.2	1124.14
5'-pGGCG (a ₅ -B)	1452.8	1453.20
5'-pGGCGC (a ₆ -B, -2)	870.7	870.62
5'-pGGCGCC (a ₇ -B, -2)	1015.7	1015.14
5'-pGGCGCCG (a ₈ -B, -2)	1179.4	1179.67
pCGCCGAGT-3' (w ₈ , -2)	1244.0	1243.70
pCCGAGT-3' (w ₆ , -2)	935.1	934.65
pAGT-3' (w ₃)	963.5	963.16
pGT-3' (w ₂)	650.1	650.10

RT: 0.00 - 17.00



NL:
1.72E8
TIC F: MS
Dpo4 N2 G1

Figure S33. LC-ESI-MS/MS analysis of the Dpo4 extension of oligonucleotide **1c**.

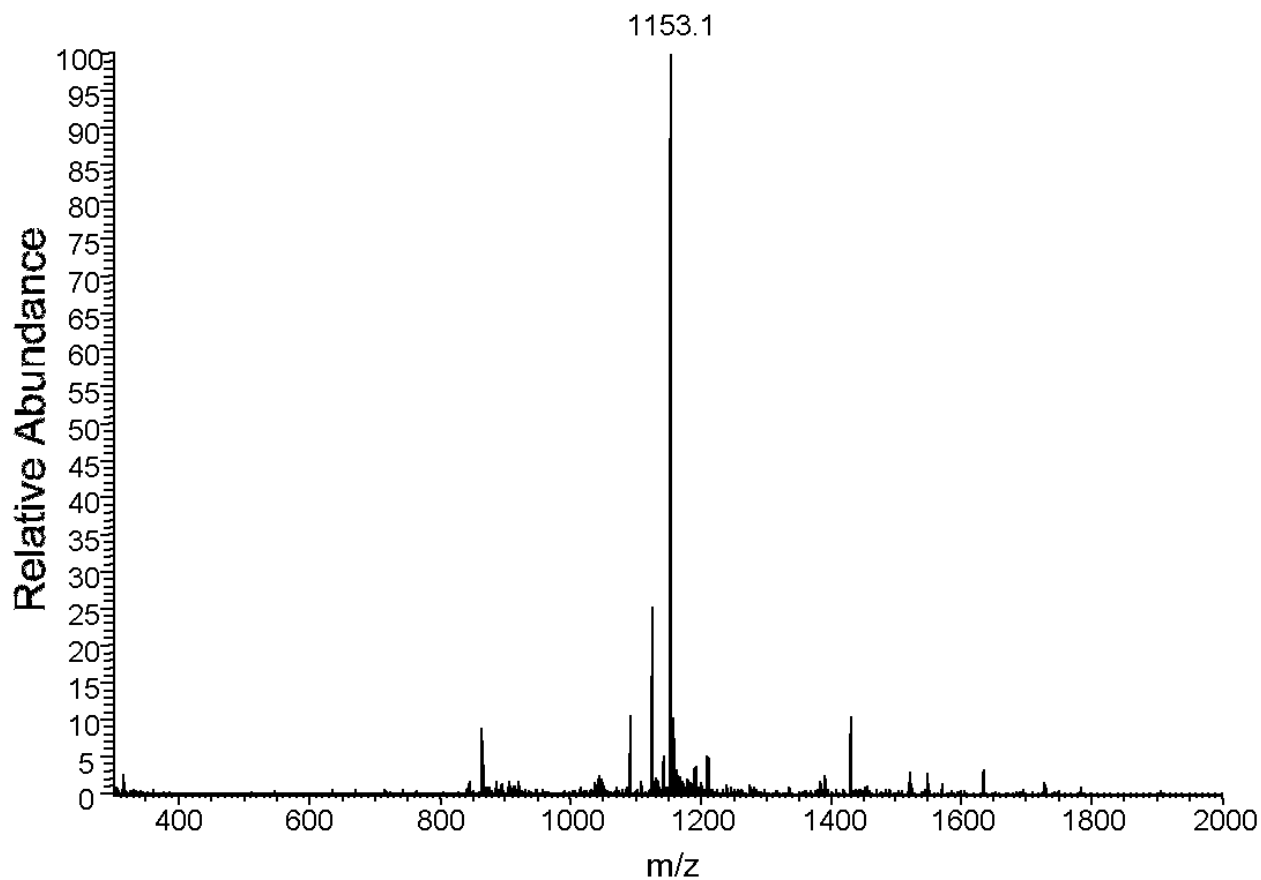


Figure S34. TIC spectrum of the Dpo4 extension products from oligonucleotide **1c**.

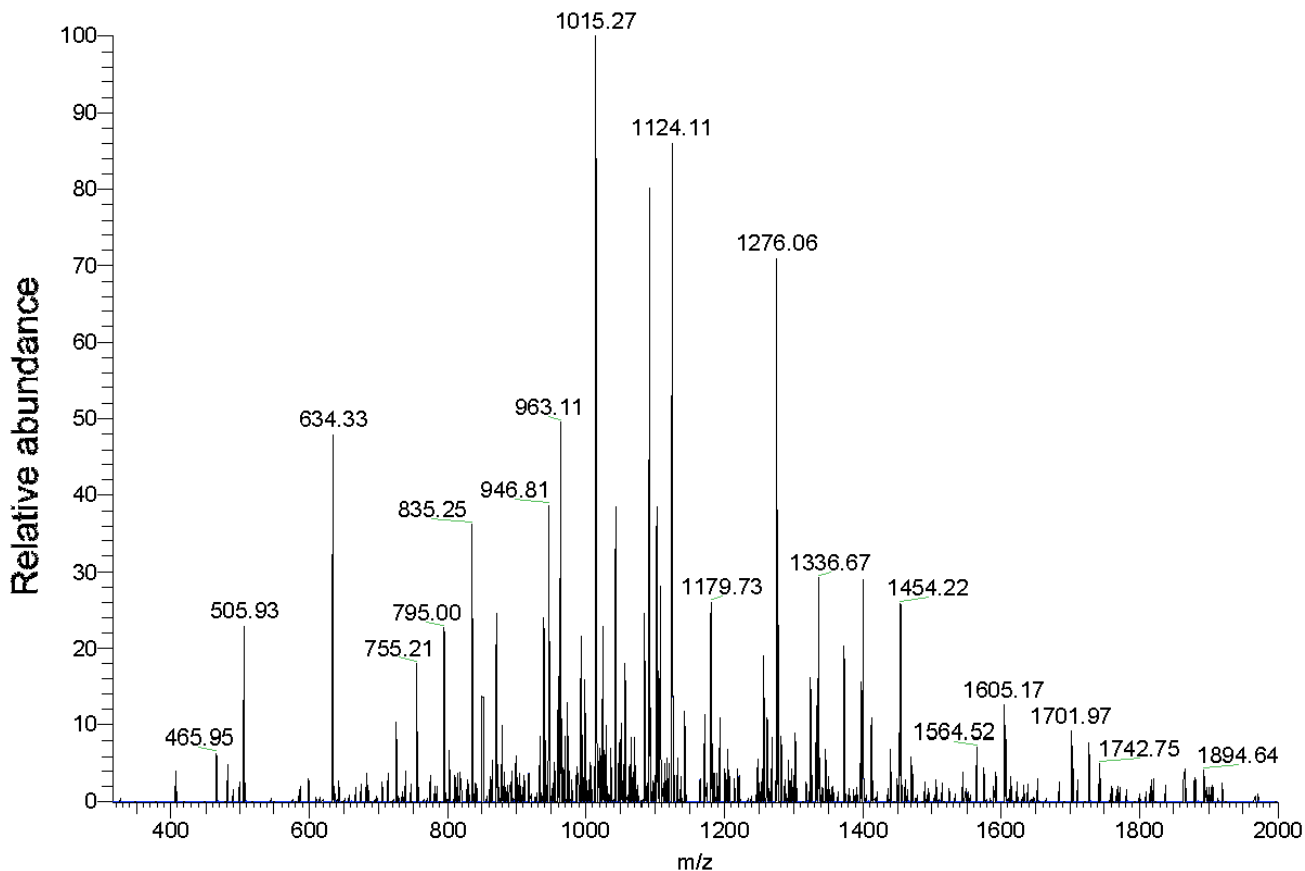


Figure S35. CID spectrum of the m/z 1153.1 products from the Dpo4 extension of oligonucleotide **1c**.

Table S7. Observed and calculated CID fragmentation of 5'-pGGCGCCGAGTA-3' (m/z 1153.1)

Fragment assignment	observed	theoretical
5'-pG (a_2 -B)	506.93	506.05
5'-pGG (a_3 -B)	835.3	835.10
5'-pGGC (a_4 -B)	1124.1	1124.14
5'-pGGCG (a_5 -B)	1454.2	1453.20
5'-pGGCGC (a_6 -B)	1742.7	1742.24
(a_6 -B, -2)	870.8	870.6
5'-pGGCGCC (a_7 -B, -2)	1015.3	1015.14
5'-pGGCGCCG (a_8 -B, -2)	1179.7	1179.67
5'-pGGCGCCGA (a_9 -B, -2)	1336.7	1336.20
pGGCGCCGAGTA-3' (w_8 , -2)	1400.7	1400.22
pCGCCGAGTA-3' (w_8 , -2)	1256.2	1255.70
pGCCGAGTA-3' (w_7 , -2)	1091.4	1091.18
pCCGAGTA-3' (w_6 , -2)	946.8	946.65
pGAGTA-3' (w_5)	1605.7	1605.27
pAGTA-3' (w_4)	1276.0	1276.21
pGTA-3' (w_3)	963.1	963.16
pTA-3' (w_2)	634.3	634.10

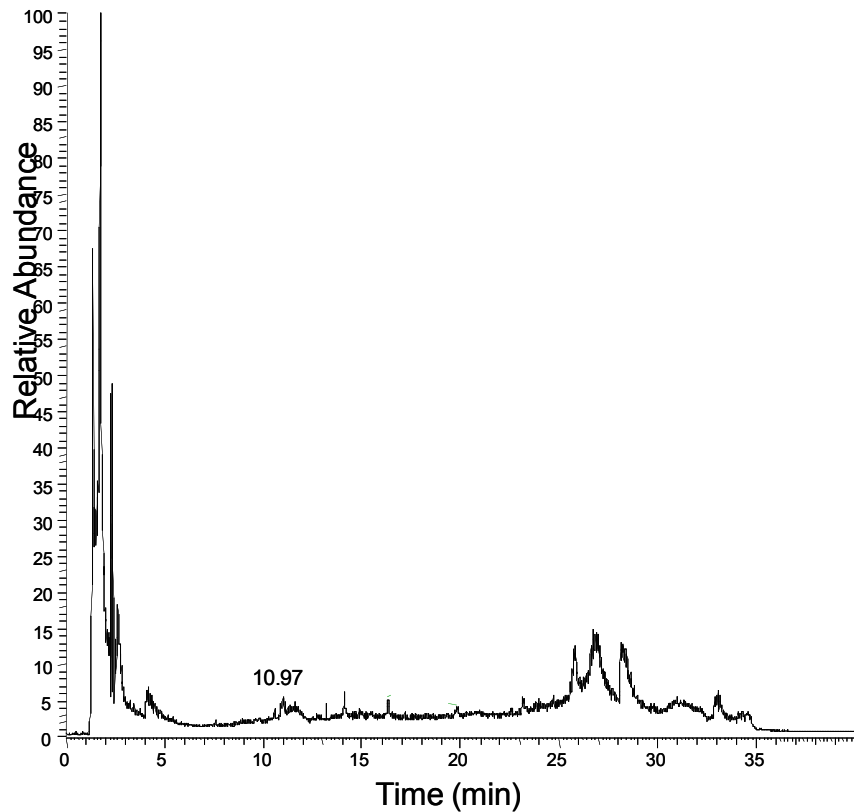


Figure S36. LC-ESI-MS/MS analysis of the Dpo4 extension of oligonucleotide **2c**.

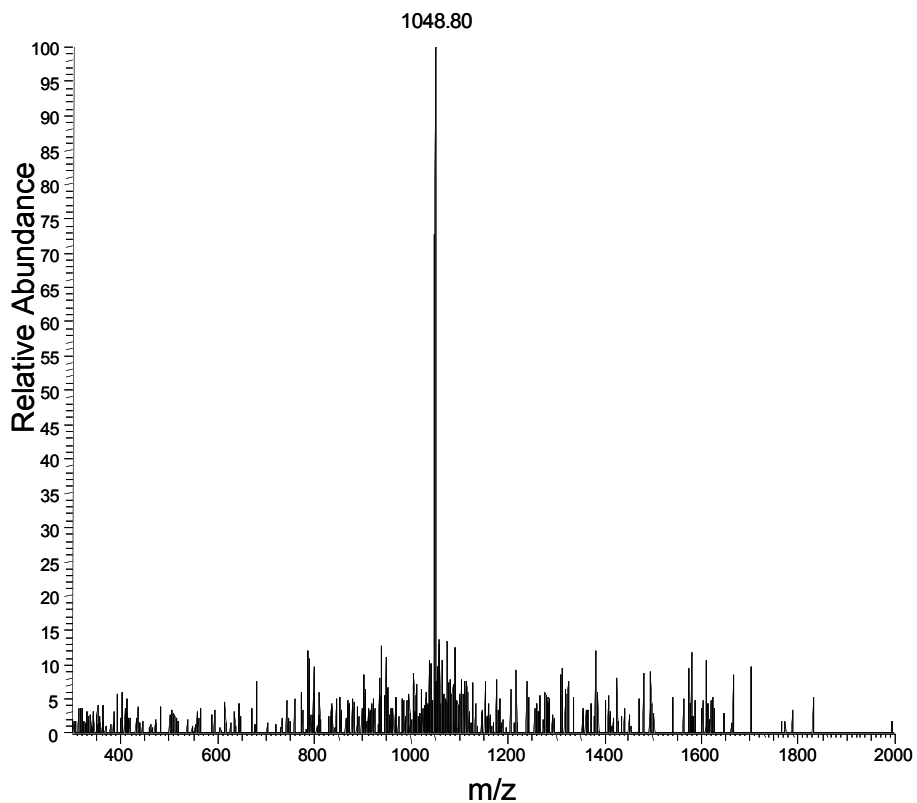


Figure S37. TIC spectrum of the Dpo4 extension products from oligonucleotide **2c**.

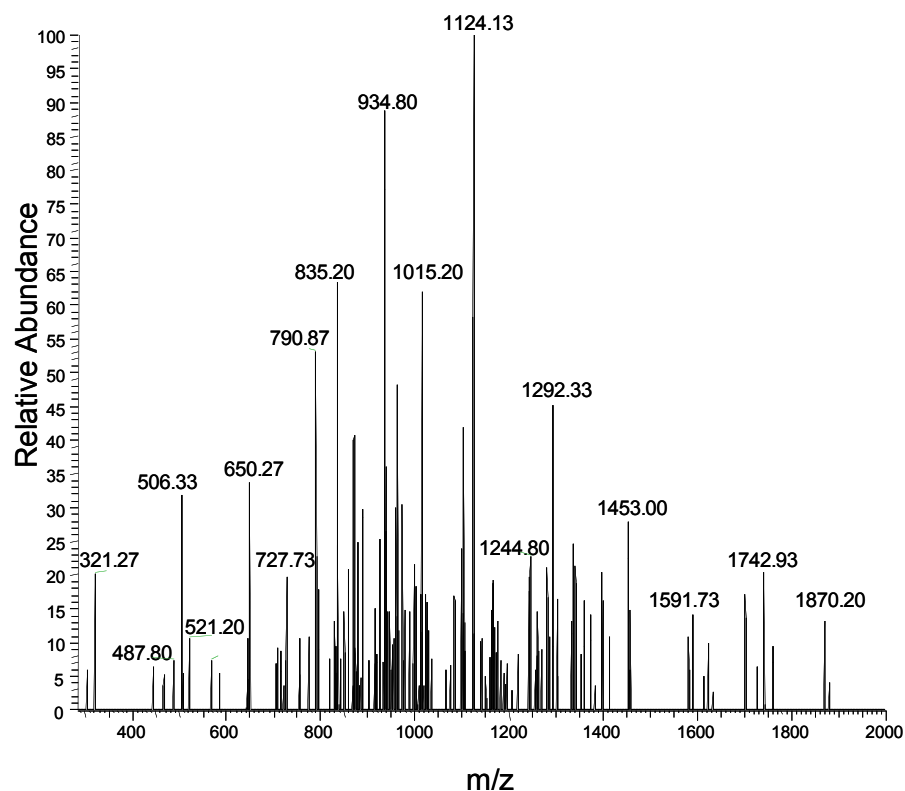


Figure S38. CID spectrum of the *m/z* xxx products from the Dpo4 extension of oligonucleotide **2b**.

Table S8. Observed and calculated CID fragmentation of 5'-pGGCGCCGAGT-3' (*m/z* 1048.8)

Fragment assignment	observed	theoretical
5'-pG (a ₂ -B)	506.3	506.05
5'-pGG (a ₃ -B)	835.2	835.10
5'-pGGC (a ₄ -B)	1124.1	1124.14
5'-pGGCG (a ₅ -B)	1453.0	1453.20
5'-pGGCGC (a ₆ -B)	1742.9	1742.24
(a ₆ -B, -2)	870.5	870.62
5'-pGGCGCC (a ₇ -B, -2)	1015.2	1015.14
pCGCCGAGT-3' (w ₈ , -2)	1244.8	1243.7
pGCCGAGT-3' (w ₇ , -2)	1099.1	1099.17
pCCGAGT-3' (w ₆)	1870.2	1870.30
(w ₆ , -2)	934.8	934.65
pCGAGT-3' (w ₅ , -2)	790.9	790.12
pGAGT-3' (w ₄)	1292.3	1292.21
pAGT-3' (w ₃)	963.4	963.16
pGT-3' (w ₂)	650.2	650.10
pT-3' (w ₁)	321.3	321.05